Journal of Applied Analysis and Computation
Volume 13, Number 1, February 2023, 198–232
Website:http://www.jaac-online.com
DOI:10.11948/20220011

A MODIFIED LESLIE-GOWER FRACTIONAL ORDER PREY-PREDATOR INTERACTION MODEL INCORPORATING THE EFFECT OF FEAR ON PREY

Narayan Mondal[1], Dipesh Barman[1], Jyotirmoy Roy[1], Shariful Alam[1] and Mohammad Sajid[2,†]

Abstract In this article, a Leslie-Gower type predator prey model with fear effect has been proposed and studied in the framework of fractional calculus in Caputo sense. The well-posedness of the system has been verified analytically. The states of stability of the possible non-negative equilibrium points have been derived. It is observed that both the fear level and memory bound of the interacting species take crucial part in determining the states of stability of the system dynamics around the co-existence equilibrium point. The fear level makes the system stable around the positive equilibrium point via two consecutive Hopf bifurcations. The higher memory of the interacting species leads to stabilization of the ecological model system whether fading memory has destabilization role in the system dynamics. The analytical representations of the bifurcation scenarios have been rigorously analyzed. Also, it has been observed that the corresponding integer order model system may experience saddle-node bifurcation depending upon the change of suitable parameter. All our observations have been captured in numerical simulation portion and detailed explanations of the outcomes of the numerical simulation have been represented.

Keywords Fear factor, Caputo derivative, fractional calculus, Hopf-bifurcation.

MSC(2010) 92D25, 92D40, 37N25.

1. Introduction

In last few decades, many researchers [10, 11, 26, 33, 41, 53, 58, 59, 61] have captured and explored the predator-prey interactions in many ways to explain various ubiquitous phenomenons of the prey-predator dynamics in the field of ecology. It is observed that the pattern of predation of prey by the predators is an important factor that regulates the system dynamics. In mathematical ecology, this factor is signified through a function which is know as functional response. Several mathematical models have rigorously analysed by considering different type of functional responses and thus revealing many important dynamical properties of the associ-

†The corresponding author. Email: msajd@qu.edu.sa (M. Sajid)
[1]Department of Mathematics, Indian Institute of Engineering Science and Technology, Shibpur, Howrah-711103, India
[2]Department of Mechanical Engineering, College of Engineering, Qassim University, Buraydah, Al Qassim, Saudi Arabia

ated predator prey system [1,14,27–29,62]. Holling type functional responses are the most typical and mostly considered predation function. Among all the Holling type functional responses, the type II functional response has been widely used due to its usefulness in predator prey kinetics [54]. The functional response is basically a sigmoidal function of prey density, which confronts that initially the predator density will increase upon the increase of prey species. But, after crossing a certain threshold the predator density will remain constant no matter how much prey species are available for predation. Another important factor in predator-prey dynamics is the mutual interference among prey and predators. Leslie [34] and Gower [35] were first in this context to formulate mathematical model by assuming that the reduction in predator species is inversely proportional to per-capita availability of its preferred food. Assuming that the environmental carrying capacity of predators is proportional to available density of prey species they represent the predator dynamics by a mathematical equation. But, when predators cannot find sufficient prey for their predation then it may become threat for predator extinction. This situation can be overcome by adding an extra term in the denominator; which is biologically known as additional food. The types of mathematical models formulated on the above assumptions are known as models based on Leslie-Gower scheme and also it is known as modified Leslie-Gower models. Here, it is to be noted that the predators follow a logistic type growth and when the carrying capacity of predators are represented by the sum of proportion of available prey density and additional food for predators; then the predators are usually considered as generalist predators. Researchers have explored several aspects of the dynamical behaviour of ecological systems using Leslie-Gower scheme [2, 15, 19, 20, 24, 42, 44].

The dominant view in researching the dynamics of predator-prey interaction is that predators can only affect prey populations by direct predation. However, both field experiments and theoretical studies indicate that the mere threat of predation has the potential to impact prey species' growth, survival, and fecundity [48,60]. In these cases, prey species display anti-predator responses in the form of behavioural, morphological, or psychological changes [16–18, 36, 37]. For example, scared prey reduces their foraging behaviour and use mechanisms such as starvation to avoid predation [16, 17]. These prey strategies have a major effect on their ability to produce offspring as well as their adult survival capability. According to studies, the psychological state of juvenile prey can be influenced by predatory threats, and the resulting change has negative consequences for their adult endurance (for example, birds respond to predatory sounds by fleeing their nest in search of a more secure location out of fear, but can return to their old haunts if the threat diminishes). Adult perseverance can benefit from these types of resistance mechanisms for avoiding predation risk, though the main proliferation is reduced as a long-term expense [16]. As a result of the possibility of predation, some prey chooses a new living space every now and then, leaving their previous one, which could have an adverse effect on the prey's lifetime genital performance. The bad choice of environment selection, i.e., the troublesome characteristic of the new territory, affects not only the generation, but also the endurance of the adults [16]. In a field experiment conducted by Zanette et al. [66] in 2011, it was discovered that the fear of predators caused a 40% decrease in fundamental proliferation of song sparrows. This drop is a result of anti-predator activity, which has an impact on both the birth and survival rates of progeny.

On the other hand, individual experiences and memories have a role in shaping

the dynamics of a system, particularly when some additional influences are prevalent. Because of several convoluted results, biological organisms have memory that is linked to their anatomy or psychology [21,22,43,49–51]. As a result, mathematical models of predator-prey systems should provide a substitute for recording the remembrance effect. Integer order calculus have been used in mathematical models to describe and understand the dynamics of many biological systems. Many ecological processes, on the other hand, have the memory effect. Differential fractional order equations have more benefits to the modelling of these processes than differential equations of integer order as fractional order refers to grasp the whole time status of a dynamic process, and derivatives of integer order can only affiliate a particular alternation or feature at a certain stage of that process. The applicability and practical importance of fractional derivatives in many different areas of mathematics and science have previously been proven [3, 4]. Numerous researchers have tracked down the adequacy of fractional derivatives in biological and progressive process, including the adaptability to organize derivatives, management of the past memory of species obtained from their life cycle, co-genital properties etc. [5, 6, 9, 25, 38]. Two species interaction model with group defence tactics was recently studied by Alidousti and Ghafari [7] with the utilization of the fractional calculus. It is found that the system's fractional order is crucial in decreasing irregular oscillations of the system. Amirian [8] investigated the dynamical qualities of a multi-animals group system with shared helpful hunters utilizing fractional calculus, and discovered that the fractional order system is more steady than the integer order counterpart.

We can find several research articles in literature that have explored the impact of predator incited fear on determining different aspects of stability of equilibrium states, emergence of bifurcation scenarios, limit cycle oscillations and other dynamical properties related to the systems [46, 55, 57, 63–65, 67]. But, notably, impact of fear on prey species induced from generalist type predators are less explored. Moreover, the influence of memory bound on such kind of predator-prey dynamics has not been yet analyzed rigorously. In this regard, we attempt to study a fractional order predator-prey model system with Leslie-Gower scheme to explore the combined memory effect of the species and fear factor on the dynamics of our proposed system. Our main target is to answer the following questions:

i) What is the role of predator induced fear in the fractional framework system dynamics when predators suffer from favourite food?

ii) What is the role of memory of interacting species of the proposed Leslie-Gower system in the system dynamics?

This article has been organized into several sections. Section 2 deals with the process of forming the proposed mathematical model while Section 3 explores some basic mathematical preliminaries of fractional calculus that are useful in this regard. Section 4 and Section 5 respectively reveal the analysis of well-posedness and stability analysis of the system. Section 6 represents the analysis of Hopf-bifurcation while Section 7 investigates the findings of this article through proper numerical simulations. Finally, the article ends with conclusion section.

2. Formulation of mathematical model

In this article, we have constructed a two species prey-predator framework whose population densities are denoted by $x(t)$ and $y(t)$ at any time t respectively. We have

considered some assumptions while constructing the proposed system as discussed below one by one:

(i) The prey population grows in logistic fashion with birth rate r due to the non-appearance of predator. The densities of prey species vanishes in two ways: **(a)** due to intraspecific competition (the parameter m) and **(b)** due to the natural mortality (the parameter d). So, the above assumptions mathematically can be expressed by the underlying differential equation:

$$\frac{dx}{dt} = (r-d)x - mx^2. \tag{2.1}$$

(ii) In this step, we have considered the predator exerted fear function to the basic reproduction of the prey population [66] by multiplying it to the growth rate of the prey species. This fear function $\Phi(k,y)$ was first proposed by X. Wang et al [63] and then many researchers D. Barman et al. [12], and N. Mondal et al [41] have used it in their research articles. However, the differential equation (2.1) reduces to in the form:

$$\frac{dx}{dt} = r\Phi(k,y)x - dx - mx^2, \tag{2.2}$$

where

$$\Phi(k,y) = \frac{1}{1+ky}. \tag{2.3}$$

Here, k means the fear factor and it is assumed that the fear function "$\Phi(k,y)$" satisfies the following properties:

(a) $\Phi(0,y) = 1$, i.e., if no such fear exists ($k = 0$), then the growth rate of prey population remains same as earlier.

(b) $\Phi(k,0) = 1$, i.e., if there is no predator population, the prey population does not experience any effect on growth rate due to fear.

(c) $\Phi(k,y) = 0$ as $k \to \infty$, i.e., the production rate of prey population decreases with respect to the increasing level of predator induced fear.

(d) $\Phi(k,y) = 0$ as $y \to \infty$, i.e., in the presence of huge number of predators the prey population sufficiently reduces their reproduction.

(e) $\dfrac{\partial \Phi(k,y)}{\partial k} < 0$, i.e., when the fear level is increased, then the growth rate of prey reduced.

(f) $\dfrac{\partial \Phi(k,y)}{\partial k} < 0$, i.e., when the predator population density is increased, then the production rate of prey population reduced.

(iii) In prey-predator ecological modelling, functional response plays an important role in determining the system dynamics. Many researchers [23, 40, 56] have taken Beddington-DeAngelis, Michaelis–Menten or Holling Type-II scheme functional response for this cause. However, for our suitability we have contemplated a Holling Type-II scheme $\left(\dfrac{cx}{a+x}\right)$, where predators consumes the prey individuals at a rate c.

(iv) According to Berryman [13], the dynamical behaviour among the predators and prey population density will be the most prevalent factor in mathematical biology due to its world-wide importance and existence. Leslie [39] shows the famous Leslie prey-predator model as bellow:

$$\begin{cases} \dfrac{dx}{dt} = (r_2 - b_1 x)\, x - P(x)y, \\ \dfrac{dy}{dt} = \left(r_3 - a_2 \dfrac{y}{x}\right) y. \end{cases} \tag{2.4}$$

Here, at any time t the intrinsic growth rates of the prey and predator populations are represented by r_2 and r_3 respectively and b_1 is the intra-species competition rate among prey species $x(t)$ itself. The predator species devoured the prey species according to the functional response $p(x)$ and $\dfrac{x}{a_2}$ is the carrying capacity. Here, a_2 denotes the amount of the food quantity that is provided by prey species which get converted to predator's birth rate. The expression $\dfrac{y}{x}$ refers to the Leslie-Gower term, which describes the loss of predator species due to the rarity (per capita $\dfrac{y}{x}$) of their preferred food. The most significant aspect in the Leslie model is that the predator's carrying capacity is related to the quantity of prey. The Lotka-Volterra model does not specify upper bounds on the rates of growth in the prey $x(t)$ and predator $y(t)$ populations, respectively. Under the following circumstances, these top limits may be approached by: (**a**) for predators when the proportion of prey per predator is high; (**b**) for prey when the frequency of predators is low and the number of prey population seems to be low as well. We anticipate that the predator's growth will be of the modified Leslie-Gower type. Daher and Aziz-Alaoui [2] looked into this matter. In the event of extreme scarcity, predator $y(t)$ may move to other populations, but its development will be constrained by the fact that its preferred prey $x(t)$ is scarce. They proposed adding a constant amount $b > 0$ (say) to the denominator of the second equation of the system (2.4) to address this kind of issue. Now, the system of equations (2.4) reduce to the modified Leslie-Gower and Holling-II type predator-prey system $\left(p(x) = \dfrac{cx}{a+x}\right)$:

$$\begin{cases} \dfrac{dx}{dt} = (r_2 - b_1 x)\, x - \dfrac{cxy}{a+x}, \\ \dfrac{dy}{dt} = \left(r_3 - a_2 \dfrac{y}{b+x}\right) y. \end{cases} \tag{2.5}$$

With the help of the expression (2.2) and (2.3), we re-modify the system of equations (2.5) to the following form:

$$\begin{cases} \dfrac{dx}{dt} = \dfrac{rx}{1+ky} - mx^2 - dx - \dfrac{cxy}{a+x}, \ x(0) > 0 \\ \dfrac{dy}{dt} = y\left(r_1 - \dfrac{fy}{b+x}\right), \ y(0) > 0. \end{cases} \tag{2.6}$$

Here, each of the parameters are always non-negative and the term $\frac{fy}{b+x}$ is the modified Leslie–Gower term, which represents a decrease in the number of the predator population due to the deficiency of its most important food.

(v) The model system (2.6) is unable to capture the influence of memory on populations due to their life cycle experiences. An ongoing ecological system, some anti-predator behaviours of prey can't be same; they would be dependent on the time bound memory of both the populations and the consequences would be analyzed accordingly. However, the above model system (2.6) have been modified into a system of fractional order differential equations in Caputo sense as bellow:

$$\begin{cases} {}^{C}_{t_0}D^{\alpha}_{t}x = \dfrac{\tilde{r}x}{1+\tilde{k}y} - \tilde{m}x^2 - \tilde{d}x - \dfrac{\tilde{c}xy}{\tilde{a}+x}, \\ {}^{C}_{t_0}D^{\alpha}_{t}y = y\left(\tilde{r_1} - \dfrac{\tilde{f}y}{\tilde{b}+x}\right). \end{cases} \tag{2.7}$$

where ${}^{C}_{t_0}D^{\alpha}_{t}$ means fractional order derivative in Caputo sense of order α, where α lies in 0 to 1 and t_0 is the non-negative initial time. Again, we see that the time dimension of left side of the system (2.7) is $(time)^{-\alpha}$ [22] but the time dimension of right side is $(time)^{-1}$. So, both dimensions are not balanced and let us convert it to the corresponding balanced system with same dimension as follows:

$$\begin{cases} {}^{C}_{t_0}D^{\alpha}_{t}x = \dfrac{\tilde{r}^{\alpha}x}{1+\tilde{k}y} - \tilde{m}^{\alpha}x^2 - \tilde{d}^{\alpha}x - \dfrac{\tilde{c}^{\alpha}xy}{\tilde{a}+x}, \\ {}^{C}_{t_0}D^{\alpha}_{t}y = y\left(\tilde{r_1}^{\alpha} - \dfrac{\tilde{f}^{\alpha}y}{\tilde{b}+x}\right). \end{cases} \tag{2.8}$$

Now, for our suitability, let us express the system (2.8) in a simplified manner as below and the model parameters are stated in the Table 1:

$$\begin{cases} {}^{C}_{t_0}D^{\alpha}_{t}x = \dfrac{rx}{1+ky} - mx^2 - dx - \dfrac{cxy}{a+x}, \ x(0) > 0 \\ {}^{C}_{t_0}D^{\alpha}_{t}y = y\left(r_1 - \dfrac{fy}{b+x}\right), \ y(0) > 0. \end{cases} \tag{2.9}$$

Table 1. Meaning of model parameters.

Parameters in Caputo Sense	is same as	Meaning of Parameters
$\tilde{r}^{\alpha}$	r	Production rate of prey population
$\tilde{k}$	k	Predator-led level of fear
$\tilde{m}^{\alpha}$	m	Intra-specific competition among prey
$\tilde{c}^{\alpha}$	c	Rate of predatory consumption
$\tilde{a}$	a	Half saturation constant
$\tilde{f}^{\alpha}$	f	Prey provides the amount of food quantity
$\tilde{b}$	b	Half-saturation constant of prey populations
$\tilde{r_1}^{\alpha}$	r_1	Birth rate of predator species
$\tilde{d}^{\alpha}$	d	Death rate of prey population

3. Mathematical preliminaries of the above model system

Here, we have discussed some definitions and lemmas, and theorems about fractional order derivative (FOD) in Caputo sense purpose.

Definition 3.1. Caputo derivative: [47] The FOD of order α for any continuous function $s(t) \in C^n\Big([t_0, +\infty), \mathbb{R}\Big)$ can be stated as bellow

$$ {}^{C}_{t_0}D^{\alpha}_{t} s(t) = \frac{1}{\Gamma(n-\alpha)} \int_{t_0}^{t} \frac{s^n(l)}{(t-l)^{\alpha-n+1}} dl, $$

where $\Gamma(n-\alpha)$ means the gamma function and n is positive integer and α lies in $(n-1) < \alpha < n$ with $t \geq t_0$. For example, $n = 1$ we have $\alpha \in (0, 1)$ which presents the mathematical form of Caputo derivative as bellow:

$$ {}^{C}_{t_0}D^{\alpha}_{t} s(t) = \frac{1}{\Gamma(1-\alpha)} \int_{t_0}^{t} \frac{s'(l)}{(t-l)^{\alpha}} dl, $$

where α is the order of the FOD.

Lemma 3.1 ([45]). *Let, $\alpha \in (0, 1]$ and the continuous function $s(t) \in C[a_1, a_2]$ along with ${}^{C}_{t_0}D^{\alpha}_{t} s(t)$ be continuous in $[a_1, a_2]$. Now, for any $t \in (a_1, a_2)$,*

(I) ${}^{C}_{t_0}D^{\alpha}_{t} s(t) \geq 0$; this demonstrates $s(t)$ is a non-decreasing function for all $t \in [a_1, a_2]$ and

(II) ${}^{C}_{t_0}D^{\alpha}_{t} s(t) \leq 0$; this demonstrates $s(t)$ is a non-increasing function for all $t \in [a_1, a_2]$.

Theorem 3.1 ([31]). *Let, $s(t)$ be n times continuously derivable function and the FOD in Caputo sense of $s(t)$, i.e., ${}^{C}_{t_0}D^{\alpha}_{t} s(t)$ is piece wise continuous on $[t_0, \infty)$ where $\alpha > 0$ and α belongs to open interval $n-1$ to n and $n \in \mathbb{N}$. Therefore, the Laplace transformation of the above defined Caputo derivative becomes*

$$ \mathcal{L}\left\{ {}^{C}_{t_0}D^{\alpha}_{t} s(t) \right\} = l^{\alpha} F(l) - \sum_{i=0}^{n-1} l^{\alpha-i-1} s^i(t_0), $$

where $F(l) = \mathcal{L}\{s(t)\}$, the convergence of Laplace transform will be satisfied if the real part $R(l)$ of the improper integral is positive, where l is the imaginary number.

Theorem 3.2 ([30]). *For any $B \in \mathbb{C}^{n \times n}$,*

$$ \mathcal{L}\left\{ t^{d-1} E_{c_1, c_2}\ (B t_1^c) \right\} = \frac{l^{c_1 - c_2}}{l_1^c - B}, $$

for every $c_1, c_2 > 0$ and $\mathcal{R}(l) > ||B||^{\frac{1}{c_1}}$, where $\mathcal{R}(l)$ is the real part of imaginary number l, and E_{c_1, c_2} stands for Mittag-Leffler function [49].

Definition 3.2 ([32]). We have introduced the dynamics of fractional order model system in Caputo sense as:

$$ {}^{C}_{t_0}D^{\alpha}_{t} s(t) = \psi(t, s), \tag{3.1} $$

where $s(t_0)$ are strictly greater zero. The steady states of the above system can be calculated from the equation $\psi(t,s)=0$. So, s^* will be the steady states of (3.1) if and only if $\psi(t,s^*)=0$.

Theorem 3.3. *Taking the dynamical system in fractional order in the following way*

$$ {}_{t_0}^{C}D_t^{\alpha}s(t)=\psi(\mathcal{S}),\ \text{where}\ \mathcal{S}(t_0)=\left(s_{t_0}^1,s_{t_0}^2,s_{t_0}^3,...s_{t_0}^n\right),\ s_{t_0}^i>0,\ \text{for}\ \ i=1,2,...n, \tag{3.2}$$

with $\alpha\in(0,1]$, $s(t)=\left(s^1(t),s^2(t)...s^n(t)\right)$ *and* $\psi(\mathcal{S}):[t_0,\infty)\to\mathbb{R}^{n\times n}$. *Each equilibrium points of the dynamical system* (3.2) *will be LAS (locally asymptotically stable) if each eigenvalues* λ *of the variational matrix* $J(\mathcal{S})=\dfrac{\partial(\psi_1,\psi_2,...\psi_n)}{\partial(s_1,s_2...s_n)}$ *calculated at the corresponding equilibrium points satisfies* $|arg(\lambda_i)|>\dfrac{\alpha\pi}{2}$.

Lemma 3.2 ([47]). *Stated the dynamical system of a fractional order in Caputo sense as bellow*

$$ {}_{t_0}^{C}D_t^{\alpha}s(t)=\psi(t,\mathcal{S}),\quad t_0>0, \tag{3.3}$$

where $\alpha\in(0,1]$, *with initial conditions* $\mathcal{S}(t_0)=\mathcal{S}_{t_0}$, $\psi(\mathcal{S}):[t_0,\infty)\times\sigma\to\mathbb{R}^{n\times n}$, $\sigma\subset\mathbb{R}^n$, *if* $\psi(t,\mathcal{S})$ *follows the local Lipschitz condition with respect to* $\mathcal{S}\in\mathbb{R}^n$, *i.e.,*

$$||\psi(t,\mathcal{S}_1)-\psi(t,\mathcal{S}_2)||\le\Omega\ ||\mathcal{S}_1-\mathcal{S}_2||,$$

then there is a unique solution on $[t_0,\infty)\times\sigma$ *of the system* (3.3) *and we have*

$$||\mathcal{S}_1(p_1,p_2,..,p_n)-\mathcal{S}_2(q_1,q_2,...,q_n)||\le\sum_{i=1}^{n}|p_i-q_i|,\ \text{for}\ i=1,2,..,n,\ \text{and}\ p_i,q_i\in\mathbb{R}.$$

4. Well-posedness

4.1. Non-negativity

Theorem 4.1. *There are always non-negative solution of proposed system* (2.9) *initiating from the point* (x_{t_0},y_{t_0}).

Proof. Suppose, the initial values of the solution of proposed system (2.9) is $X(t_0)=\left(x(t_0),y(t_0)\right)\in\sigma^+=\Big\{(x,y)\in\{\sigma^+:\text{where } x(t) \text{ and } y(t) \text{ both are positive real numbers }\}\Big\}$. Now, we have observed that $\exists$ a constant t_1 satisfying $t_0\le t<t_1$ such that

$$x>0,\ \text{when}\ t_0\le t<t_1,\ x(t_1)=0,\ \text{and}\ \ x(t_1^+)<0.$$

Clearly, from the system (2.9), we get

$$ {}_{t_0}^{C}D_t^{\alpha}x(t)|_{x(t_1)=0}=0.$$

Thus, by lemma (3.1), we can write $x(t_1^+)=0$, which contradicts $x(t_1^+)<0$. So, $x(t)\ge0,\ \forall\ t\in[t_0,\infty)$. In the same way, we can prove that $y(t)\ge0$, for all $t\in[t_0,\infty)$. Therefore, all solutions of (2.9) are always non-negative initiating from (x_{t_0},y_{t_0}). □

4.2. Boundedness

Theorem 4.2. *Every solutions of the system* (2.9) *are always bounded in the region* D *initiating from point* (x_{t_0}, y_{t_0}).

Proof. Let $G(t)$ be the function by adding the densities of prey $x(t)$ and predator $y(t)$. Therefore, we have

$$G = x(t) + y(t).$$

Applying Caputo derivative on $G(t)$, we have

$${}^{C}_{t_0}D^{\alpha}_{t}G(t) = \frac{rx}{1+ky} - mx^2 - dx - \frac{cxy}{a+x} + r_1 y - \frac{fy^2}{b+x}.$$

Now, for any real $\Lambda \in (-\infty, \infty)$, we must have

$${}^{C}_{t_0}D^{\alpha}_{t}G(t) + \Lambda G(t) = \frac{rx}{1+ky} - mx^2 - dx - \frac{cxy}{a+x} + r_1 y - \frac{fy^2}{b+x} + \Lambda(x+y)$$

$$\text{i.e., } {}^{C}_{t_0}D^{\alpha}_{t}G(t) + \Lambda G(t) \leq \Big(- mx^2 + (r - d + \Lambda)x - fy^2 + (r_1 + \Lambda)y\Big).$$

Therefore, the maximum value of $\Big(- mx^2 + (r - d + \Lambda)x - fy^2 + (r_1 + \Lambda)y\Big)$ is $\frac{(r-d+\Lambda)^2}{4m} + \frac{(r_1+\Lambda)^2}{4f}$. So,

$${}^{C}_{t_0}D^{\alpha}_{t}G(t) + \Lambda G(t) \leq \frac{(r-d+\Lambda)^2}{4m} + \frac{(r_1+\Lambda)^2}{4f}. \tag{4.1}$$

Now, using Theorem (3.1) and taking Laplace transform on both sides of (4.1), we get

$$l^{\alpha}F(l) - l^{\alpha-1}G(0) + dF(l) \leq \frac{(r-d+\Lambda)^2}{4m} + \frac{(r_1+\Lambda)^2}{4f}\frac{1}{s}, \quad \text{where } F(l) = \mathcal{L}\{G(t)\}$$

$$[l^{\alpha+1} + dl]F(l) \leq l^{\alpha}G(0) + W, \quad \text{where } W = \frac{(r-d+\Lambda)^2}{4m} + \frac{(r_1+\Lambda)^2}{4f}$$

$$F(l) \leq G(0)\frac{l^{\alpha-1}}{l^{\alpha}+d} + \frac{W}{l(l^{\alpha}+d)}. \tag{4.2}$$

Again, applying both sides $\mathcal{L}^{-1}$ of the expression (4.2)

$$G(t) \leq G(0)\mathcal{L}^{-1}\left\{\frac{l^{\alpha-1}}{l^{\alpha}+d}\right\} + W\mathcal{L}^{-1}\left\{\frac{l^{\alpha-(\alpha+1)}}{l^{\alpha}+d}\right\}. \tag{4.3}$$

Now, using Theorem 3.2, the equation (4.3) reduces in the following form

$$G(t) \leq G(0)\ E_{\alpha,1}\{-dt^{\alpha}\} + Wt^{\alpha}E_{\alpha,\alpha+1}\{-dt^{\alpha}\}. \tag{4.4}$$

From Mittag-Leffler function, we can write

$$E_{\alpha,1}\{-dt^{\alpha}\} = (-dt^{\alpha})E_{\alpha,\alpha+1}\{-dt^{\alpha}\} + \frac{1}{\Gamma(1)}$$

$$t^{\alpha}E_{\alpha,\alpha+1}\left\{-dt^{\alpha}\right\} = -\frac{1}{d}\left[E_{\alpha,1}\left\{-dt^{\alpha}\right\} - 1\right]. \tag{4.5}$$

Therefore, using the relation (4.5), the inequality (4.4) reduces to the form

$$G(t) \leq \left\{G(0) - \frac{W}{d}\right\} E_{\alpha,1}\left\{-dt^{\alpha}\right\} + \frac{W}{d}. \tag{4.6}$$

For, $E_{\alpha,1}$ tends to 0 as t tends to $+\infty$. So,

$$G(t) \leq \frac{W}{d} = \frac{(r-d+\Lambda)^2}{4m} + \frac{(r_1+\Lambda)^2}{4f}.$$

Hence, each solutions of the system (2.9) are always bounded in the region

$$D = \left\{(x(t), y(t)) \in \sigma^{+} |\ 0 < (x(t)+y(t)) \leq \frac{(r-d+\Lambda)^2}{4m} + \frac{(r_1+\Lambda)^2}{4f} + \delta, \delta > 0\right\}.$$

□

4.3. Existence and uniqueness

Theorem 4.3. *There exists always unique solution in σ_+ of the system (2.9) by taking the initial value $(x_{t_0}, y_{t_0}) \in \sigma_+$, $\forall\ t \geq t_0$.*

Proof. Let us assume the interval $t_0 \leq t \leq t_1$, where $t_1 < +\infty$ and the region $\sigma_+ = \left\{(x,y) \in \mathbb{R}^2_+ |\ \max\{|x|,|y|\} \leq N\right\}$. Now, again consider the mapping $\tilde{T}(X) = \left(\tilde{T}_1(X), \tilde{T}_2(X)\right)^t$, where $X = (x,y)^t$ and

$$\tilde{T}_1(X) = \frac{rx}{1+ky} - mx^2 - dx - \frac{cxy}{a+x},$$
$$\tilde{T}_2(X) = r_1 y - \frac{fy^2}{b+x}.$$

Now, for $X, \bar{X} \in \sigma_+$, we get

$$\begin{aligned}
&||\tilde{T}(X) - \tilde{T}(\bar{X})|| \\
&= |\tilde{T}_1(X) - \tilde{T}_1(\bar{X})| + |\tilde{T}_2(X) - \tilde{T}_2(\bar{X})| \\
&= \left|\frac{rx}{1+ky} - mx^2 - dx - \frac{cxy}{a+x} - \frac{r\bar{x}}{1+k\bar{y}} + m\bar{x}^2 + d\bar{x} + \frac{c\bar{x}\bar{y}}{a+\bar{x}}\right| \\
&\quad + \left|r_1 y - \frac{fy^2}{b+x} - r_1\bar{y} + \frac{f\bar{y}^2}{b+\bar{x}}\ \right| \\
&= \left|\frac{\Big(r(x-\bar{x}) + rk(x\bar{y} - \bar{x}y)\Big)}{(1+ky)(1+k\bar{y})} - m(\bar{x}+x)(x-\bar{x}) - d(x-\bar{x}) + \frac{ac(\bar{x}\bar{y} - xy) - cx\bar{x}(y-\bar{y})}{(a+x)(a+\bar{x})}\right| \\
&\quad + \left|r_1(y-\bar{y}) - \Big(\frac{fy^2(b+\bar{x}) - f\bar{y}^2(b+x)}{(b+x)(b+\bar{x})}\Big)\ \right| \\
&\leq \big|r(x-\bar{x}) + rk\{\bar{y}(x-\bar{x}) - \bar{x}(y-\bar{y})\} - m(\bar{x}+x)(x-\bar{x}) - d(x-\bar{x}) \\
&\quad - ac\{y(x-\bar{x}) + \bar{x}(y-\bar{y})\} - cx\bar{x}(y-\bar{y})\ \big|
\end{aligned}$$

$$
\begin{aligned}
&+ \left|r_1(y-\bar{y}) - fb(y+\bar{y})(y-\bar{y}) + f\bar{y}^2(x-\bar{x}) - f\bar{x}(y+\bar{y})(y-\bar{y})\right| \\
&\leq [r + rkN + 2mN + d + acN + N^2]|x-\bar{x}| \\
&\quad + [rkN + acN + cN^2 + r_1 + 2fN + 2fN^2]|y-\bar{y}| \\
&= K_1|x-\bar{x}| + K_2|y-\bar{y}| \\
&\leq K||X-\bar{X}||
\end{aligned}
$$

where $K = \max\{K_1, K_2\}$ with $K_1 = [r + rkN + 2mN + d + acN + N^2]$ and $K_2 = [rkN + acN + cN^2 + r_1 + 2fN + 2fN^2]$. So, the local Lipschitz condition holds and hence the system (2.9) possesses unique solution. □

5. Stability analysis of equilibria

5.1. Equilibria and their existence criteria

The proposed system (2.9) has four possible steady states, they are

(I) The trivial equilibrium point $E_{s0}(0,0)$,

(II) $E_{s1}\left(\dfrac{r-d}{m}, 0\right)$, i.e., axial or predator free steady state exists under the condition $r > d$, i.e., E_{s1} exists if the birth rate of prey species is strictly greater than its death rate.

(III) The another axial point $E_{s2}\left(0, \dfrac{r_1 b}{f}\right)$ always exists without any parametric restrictions.

(IV) The interior equilibrium pint $E_{s*}(x^*, y^*)$ whose first component can be found from the following equation:

$$x^* = \left(\frac{fy^*}{r_1} - b\right) \tag{5.1}$$

and second component can be obtained from the equation (5.2):

$$\delta_{11}(y^*)^3 + \delta_{12}(y^*)^2 + \delta_{13}(y^*) + \delta_{14} = 0, \tag{5.2}$$

where

$$
\begin{aligned}
\delta_{11} &= \frac{mkf^2}{r_1^2}, \\
\delta_{12} &= ck + \frac{dkf}{r_1} - \frac{3bmkf}{r_1}, \\
\delta_{13} &= c + adk + mkb^2 + \frac{df}{r_1} + \frac{amf}{r_1} + \frac{mf^2}{r_1^2} + \frac{amfk}{r_1} - \frac{fr}{r_1} - \frac{2bmf}{r_1} - abmk - bdk, \\
\delta_{14} &= ad + br + mb^2 - ar - abm - bd.
\end{aligned}
$$

Since the equation (5.2) is of degree 3, so it has at least one real solution. Here, δ_{11} is strictly greater than zero. The equation (5.2) will have a positive solution and the existence conditions of interior steady state can be stated as follows:

(a) If $\delta_{12} < 0$, i.e., if $r_1c + df < 3bmf$, then the equation (5.2) has positive root say, $y^* = \beta_1$ and from (5.1) we have $x^* = \left(\frac{f\beta_1}{r_1} - b\right)$. So it exists if $\beta_1 > \frac{br_1}{f}$.

(b) Similarly, if $\delta_{13} < 0$, i.e., if $(cr_1 + adkr_1 + mb^2kr_1 + df + amf + mf^2 + akmf) < (fr + 2bmf + abmkr_1 + bdkr_1)$, then the (5.2) has positive root $y^* = \beta_2 > 0$ (say) and from (5.1) we get $x^* = \left(\frac{f\beta_2}{r_1} - b\right)$. It exists if $\beta_2 > \frac{br_1}{f}$.

(c) Again similarly, if $\delta_{14} < 0$, i.e., if $(ad + br + mb^2) < (ar + abm + bd)$, then the (5.2) has positive root say $y^* = \beta_3 > 0$ and from (5.1) we have $x^* = \left(\frac{f\beta_3}{r_1} - b\right)$. Now, if $\beta_3 > \frac{br_1}{f}$, then x^* is strictly greater than zero.

5.2. Stability Analysis

In this portion, we have investigated the local stability conditions of each equilibrium points in the following theorems one by one. For this purpose, we have calculated the variational matrix as follows:

$$J_v(x,y) = \begin{pmatrix} \frac{r}{1+ky} - 2mx - d - \frac{acy}{(a+x)^2} & -\frac{kx}{(1+ky)^2} - \frac{cx}{a+x} \\ \frac{fy^2}{(b+x)^2} & r_1 - \frac{2fy}{b+x} \end{pmatrix}.$$

Theorem 5.1. *There is no parametric restriction of the trivial point $E_{s0}(0,0)$ and it will be always unstable.*

Proof. The variational matrix of the system (2.9) at $E_{s0}(0,0)$ is

$$J_0(E_{s0}(0,0)) = \begin{pmatrix} r-d & 0 \\ 0 & r_1 \end{pmatrix}.$$

Clearly, the eigenvalues of the variational matrix $J_0(E_{s0})$ are $\lambda_1 = r-d$ and $\lambda_2 = r_1$. When $r \geq d$ and $\lambda_2 = r_1 > 0$, then, λ_1 is non$-$negative real number and λ_2 is positive number which implies that

$$|amp(\lambda_i)| \text{ or } |arg(\lambda_i)| = 0 < \frac{\alpha\pi}{2} \text{ for } i = 1, 2.$$

Therefore, $E_{s0}(0,0)$ is always unstable. If $r < d$, then λ_1 must be negative real number.

$$|arg(\lambda_1)| = \pi > \frac{\alpha\pi}{2} \text{ and } |arg(\lambda_2)| = 0 < \frac{\alpha\pi}{2}.$$

Similarly, $E_{s0}(0,0)$ will be saddle point and it is unstable. □

Theorem 5.2. *The system* (2.9) *displays the unstable scenario around the predator free equilibrium point $E_{s1}\left(\frac{r-d}{m}, 0\right)$ without any parametric condition.*

Proof. The characteristic equation corresponding the Jacobian matrix at $E_{s1}(\frac{r-d}{m}, 0)$ is

$$\{\lambda + (r-d)\}\{\lambda - r_1\} = 0.$$

This shows $\lambda_1 = -(r-d)$ and $\lambda_2 = r_1$. Already it was known that $r > d$ from the existence criteria of predator free equilibrium point and obviously, λ_1 must be negative real number and $\lambda_2 > 0$. Then

$$|arg(\lambda_1)| = \pi > \frac{\alpha\pi}{2} \quad \text{and} \quad |arg(\lambda_2)| = 0 < \frac{\alpha\pi}{2}.$$

Thus, the equilibrium point $E_{s1}\left(\frac{r-d}{m}, 0\right)$ will be saddle point and it is always unstable. □

Theorem 5.3. *The another prey free equilibrium point* $E_{s2}\left(0, \frac{br_1}{f}\right)$ *of the system* (2.9) *will be asymptotically stable if* $\frac{rf}{f+bkr_1} < d + \frac{bcr_1}{af}$ *and otherwise the axial equilibrium point will be unstable.*

Proof. The characteristic equation of the above Jacobian matrix of the system (2.9) at $E_{s2}\left(0, \frac{br_1}{f}\right)$ is

$$\left\{\lambda - \left(\frac{rf}{f+bkr_1} - \frac{bcr_1}{af} - d\right)\right\}\Big\{\lambda + r_1\Big\} = 0.$$

The eigenvalues are $\lambda_1 = \frac{rf}{f+bkr_1} - d - \frac{bcr_1}{af}$ and $\lambda_2 = -r_1$. Here, $r_1 > 0$ and when $\frac{rf}{f+bkr_1} < d + \frac{bcr_1}{af}$, then the two eigenvalues are negative. Thus,

$$|arg(\lambda_i)| = \pi > \frac{\alpha\pi}{2} \quad \text{for} \quad i = 1, 2.$$

Theorem 3.3 is satisfied by the two eigenvalues and the above said condition. We conclude that the equilibrium point $E_{s2}\left(0, \frac{br_1}{f}\right)$ becomes asymptotically stable otherwise it is unstable. This is the complete proof of this theorem. □

Theorem 5.4. *The system* (2.9) *exhibits stable scenario around the interior steady state* $E_{s*}(x^*, y^*)$ *if the following conditions hold:*

(i) $e_{13} \leq 0$ *and*

(ii) $e_{13} > 0, e_{13}^2 - 4e_{14} < 0$ *and* $e_{15} > e_{13}\ tan\left(\frac{\alpha\pi}{2}\right)$*, otherwise the above axial equilibrium point is unstable.*

Proof. The Jacobian matrix corresponding to the interior steady state $E_{s*}(x^*, y^*)$ is

$$J(E_{s*}(x^*, y^*)) = \begin{pmatrix} e_{11} & e_{12} \\ e_{21} & e_{22} \end{pmatrix},$$

where

$$e_{11} = \frac{r}{1+ky^*} - 2mx* - d - \frac{acy^*}{(a+x^*)^2},$$
$$e_{12} = -\frac{kx^*}{(1+ky^*)^2} - \frac{cx^*}{(a+x^*)}, e_{21} = \frac{fy^{*2}}{(b+x^*)^2},$$
$$e_{22} = r_1 - \frac{2fy^*}{b+x^*}.$$

The characteristic equation of the above variational matrix corresponding to the interior point E_s* is

$$\begin{cases} \lambda^2 - \lambda(e_{11}+e_{22}) + e_{11}e_{22} - e_{12}e_{21} = 0, \\ \text{or} \quad \lambda^2 - \lambda e_{13} + e_{14} = 0. \end{cases} \tag{5.3}$$

where $e_{13} = e_{11} + e_{22}, e_{14} = e_{11}e_{22} - e_{12}e_{21}$. The roots are

$$\lambda_{1,2} = \frac{e_{13} \pm \sqrt{e_{13}^2 - 4e_{14}}}{2}. \tag{5.4}$$

Here, we consider two cases:
CASE I: When $e_{13} \leq 0$, in this case we consider the three subcases as bellow:
Subcase I(a): $e_{13} = 0$.
Now if $e_{13} = 0$, then we have $\lambda_{1,2} = \pm i\sqrt{e_{14}}$, i.e., both eigenvalues are complex conjugate. Therefore,

$$|arg(\lambda_i)| = \frac{\pi}{2} > \frac{\alpha\pi}{2} \quad \text{for} \quad i = 1, 2,$$

and this two eigenvalues satisfies the properties of Theorem 3.3. Near this interior equilibrium point the system (2.9) shows stable scenario.
Subcase I(b): $e_{13} < 0$ and $(e_{13}^2 - 4e_{14}) \geq 0$.
We noticed that the two eigenvalues are negative after some algebric calculation. Hence,

$$|arg(\lambda_i)| = \pi > \frac{\alpha\pi}{2} \quad \text{for} \quad i = 1, 2.$$

This condition is satisfied using the Theorem 3.3 and the system (2.9) displays the stable scenario.
Subcase I(c): $e_{13} < 0$ and $(e_{13}^2 - 4e_{14}) < 0$.
In this portion, we observe that the Jacobian matrix at $E_{s*}(x^*, y^*)$ must have a pair of complex conjugate eigenvalues with negative real part. So,

$$|arg(\lambda_i)| > \frac{\alpha\pi}{2} \quad \text{for} \quad i = 1, 2.$$

Similarly, using Theorem 3.3 it can be concluded that the system (2.9) displays the stable scenario near the interior equilibrium point $E_{s*}(x^*, y^*)$.
CASE II: $e_{13} > 0$ and $(e_{13}^2 - 4e_{14}) < 0$ and $e_{15} > e_{13}\ tan\left(\frac{\alpha\pi}{2}\right)$ where, $e_{15} = \sqrt{4e_{14} - e_{13}}$. Here, we take a pair of imaginary conjugate eigenvalues that satisfy the following relation

$$\text{Imaginary part of } (\lambda_1) = -\text{Imaginary part of } (\lambda_2) = \frac{1}{2}\left(\sqrt{4e_{14} - e_{13}^2}\right) > 0$$

and Real part of $(\lambda_1) = -$Real part of $(\lambda_2) = \frac{e_{13}}{2}$.

Therefore,

$$\text{Imaginary part of } (\lambda_1) > \text{Real part of}(\lambda_1)\ \tan\left(\frac{\alpha\pi}{2}\right) \text{ and}$$
$$-\text{Imaginary part of } (\lambda_2) > \text{Real part of}(\lambda_2)\ \tan\left(\frac{\alpha\pi}{2}\right).$$

This shows

$$\frac{\alpha\pi}{2} < \arg(\lambda_1) < \frac{\pi}{2} \quad \text{and} \quad -\frac{\pi}{2} < \arg(\lambda_2) < -\frac{\alpha\pi}{2}.$$

Combining these two results, we have

$$|\arg(\lambda_i)| > \frac{\alpha\pi}{2}.$$

So, we must conclude that the system (2.9) exhibits the stable scenario near this interior equilibrium point E_{s*}. Hence the theorem is proven. □

Theorem 5.5. *Near the interior equilibrium point E_{s*} the system* (2.9) *displays unstable scenario if the following conditions hold:*

(a) $e_{13} > 0$ *and* $e_{13}^2 - 4e_{14} \geq 0$,

(b) $e_{13} > 0, e_{13}^2 - 4e_{14} < 0$ *and* $e_{15} < e_{13}\ tan\left(\frac{\alpha\pi}{2}\right)$.

Proof. Here, we consider two vital cases:
CASE-I: $e_{13} > 0$ and $e_{13}^2 - 4e_{14} \geq 0$. So, both the eigenvalues must be positive.

$$|arg(\lambda_i)| = 0 < \frac{\alpha\pi}{2} \quad \text{for} \quad i = 1, 2.$$

With help of the Theorem 3.3, the proposed system (2.9) shows the unstable scenario near the interior steady state E_{s*}.
CASE-II: $e_{13} > 0$ and $e_{13}^2 - 4e_{14} < 0$ and $e_{15} < e_{13}\ tan\left(\frac{\alpha\pi}{2}\right)$. In this case, we found a pair of imaginary conjugate eigenvalues $\lambda_1 = \bar{\lambda_2}, \lambda_2 = \bar{\lambda_1}$ such that Imaginary part of λ_1=- Imaginary part of λ_2=$\frac{1}{2}e_{15} > 0$. So we have

$$|\arg(\lambda_i)| = \tan^{-1}\left(\frac{e_{15}}{e_{13}}\right) < \frac{\alpha\pi}{2} \quad \text{for} \quad i = 1, 2.$$

Now, using the Theorem 3.3, we have concluded that the model system (2.9) is unstable close to the interior equilibrium E_{s^*}.

Hence, the theorem is completed. □

6. Bifurcation analysis

6.1. For integer-order system

6.1.1. Trans-critical bifurcation analysis

Now, let us talk about what happens when $\frac{rf}{f + bkr_1} = d + \frac{bcr_1}{af}$ **?** This is a question that arises from Theorem 5.3. Now, for this condition $\frac{rf}{f + bkr_1} = d + \frac{bcr_1}{af}$, we

could not say anything about the dynamical behavior near the axial steady state $E_{s2}\left(0, \frac{br_1}{f}\right)$ because one eigenvalue of $J(E_{s2})$ at E_{s2} is zero. Using Sotomayors theorem [52] we can state the following theorem about the dynamical behavior around the axial steady state E_{s2}.

Theorem 6.1. *The integer order model system* (2.9) *undergoes a Trans-critical bifurcation w.r.t. predator induced fear level* k *at* $k = k^{TB} = \frac{f}{br_1}\left[\frac{afr - adf - bcr_1}{adf + bcr_1}\right]$.

Proof. Let, $H = \begin{pmatrix} h_1 \\ h_2 \end{pmatrix} = \begin{pmatrix} \frac{rx}{1+ky} - mx^2 - dx - \frac{cxy}{a+x} \\ y\left(r_1 - \frac{fy}{b+x}\right) \end{pmatrix}$.

Now, for $\frac{rf}{f + bkr_1} = d + \frac{bcr_1}{af}$, i.e., at $k = k^{TB} = \frac{f}{br_1}\left[\frac{afr - adf - bcr_1}{adf + bcr_1}\right]$, the variational matrix $J(E_{s2})$ reduces to the form

$$J(E_{s2}) = \begin{pmatrix} 0 & \frac{r^2{}_1}{f} \\ 0 & -r_1 \end{pmatrix}.$$

Let $B = \begin{pmatrix} b_1 \\ b_2 \end{pmatrix}$ and $A = \begin{pmatrix} a_1 \\ a_2 \end{pmatrix}$ be the eigenvectors of $J(E_{s2}, k^T B)$ and $J^T(E_{s2}, k^T B)$ w.r.t. the zero eigenvalue respectively. After several algebraic calculations, we get $B = \begin{pmatrix} 1 \\ 0 \end{pmatrix}$ and $A = \begin{pmatrix} 1 \\ \frac{r_1}{f} \end{pmatrix}$. The integer order system (2.9) undergoes a Trans-critical bifurcation under the following conditions that obtained from Sotomayor's theorem [52]:

(i) $A^T H_k\left(E_{s2}, k^{TB}\right) = 0$,

(ii) $A^T\left[DH_k\left(E_{s2}, k^{TB}\right) B\right] \neq 0$,

(iii) $A^T\left[D^2 H_k\left(E_{s2}, k^{TB}\right)(B \;\; B)\right] \neq 0$.

Now, let us check the above restrictions one by one.
Therefore,

$$(i) \qquad A^T H_k\left(E_{s2}, k^{TB}\right)$$
$$= \begin{pmatrix} 1 & \frac{r_1}{f} \end{pmatrix}\left[\frac{rx}{1+ky} - mx^2 - dx - \frac{cxy}{a+x} y\left(r_1 - \frac{fy}{b+x}\right)\right]\Bigg|_{(E_{s2}, k^{TB})}$$
$$= \left[\frac{rx}{1+ky} - mx^2 - dx - \frac{cxy}{a+x} + \left(r_1 y - \frac{fy^2}{b+x}\right)\frac{r_1}{f}\right]\Bigg|_{(E_{s2}, k^{TB})} = 0.$$

$$(ii) \qquad A^T\left[DH_k\left(E_{s2}, k^{TB}\right) B\right]$$

$$= \left[a_1 b_1 \frac{\partial^2 h_1}{\partial x \partial k} + a_1 b_2 \frac{\partial^2 h_1}{\partial y \partial k} + a_2 b_1 \frac{\partial^2 h_2}{\partial x \partial k} + a_2 b_2 \frac{\partial^2 h_2}{\partial y \partial k}\right]\Bigg|_{(E_{s2}, k^{TB})}$$
$$= -\frac{bfrr_1}{(f + bkr_1)^2} \neq 0.$$

Finally, we obtain

$$(iii) \qquad A^T \left[D^2 H_k \left(E_{s2}, k^{TB}\right)(B \quad B)\right]\Big|_{(E_{s2}, k^{TB})}$$
$$= \left[b_1^2 \frac{\partial^2 h_2}{\partial x^2} + b_1 \frac{\partial^2 h_2}{\partial x \partial y} + b_1 \frac{\partial^2 h_2}{\partial y \partial x} + \frac{\partial^2 h_2}{\partial y^2}\right]\Bigg|_{(E_{s2}, k^{TB})}$$
$$= \frac{1}{bf}\left[4fr_1 - 2f^2 - 2r_1^2\right] = -\frac{2}{bf}(r_1 - f)^2 \neq 0.$$

Hence, all the restrictions of Sotomayor's theorem [52] are verified. So, the proof of this theorem is complete. □

6.1.2. Hopf-bifurcation analysis

Theorem 6.2. *The necessary and sufficient conditions for the occurrence of Hopf-bifurcation around the co-existence steady state $E_{s^*}(x^*, y^*)$ w.r.t. the predator induced fear parameter k is that, there exist a critical point at $k = k^*$ for which $e_{11}(k^*) + e_{22}(k^*) = 0$.*

Proof. For performing Hopf-bifurcation analysis, the variational matrix around the co-existence steady state $E_{s^*}(x^*, y^*)$ need to have a pair of complex conjugate eigenvalues whose real part changes sign under the variation of the parameter k and crosses the imaginary axis with non-zero speed. Equation (5.3) exhibits that it has a pair of purely complex eigenvalues if trace of $J(E_{s^*}(x^*, y^*)) = e_{11}(k^*) + e_{22}(k^*) = 0$ and $\Delta_{det} = (e_{11}e_{22} - e_{12}e_{21}) > 0$.

Therefore, for co-existence of Hopf point equation (5.3) turns into the following form

$$\lambda^2 + \Delta_{det}(k) = 0.$$

Thus, the both complex eigenvalues are $\lambda_{1,2} = \pm i\omega_k$ where $\omega_k = \sqrt{\Delta_{det}(k)}$. Now, we shall show that the transversality condition for which the eigenvalues just cross the imaginary axis with non-zero speed. For this issue, we have taken $k \in (k - \epsilon_1, k + \epsilon_2)$ and $\lambda_{1,2} = \zeta_1(k) \pm i\zeta_2(k)$, where $\zeta_1(k) = \frac{1}{2}[e_{11}(k) + e_{22}(k)]$ and $\zeta_2(k) = \sqrt{\Delta_{det}^2(k) - \frac{(e_{11}(k) + e_{22}(k))^2}{4}}$. Again

$$\frac{d}{df}[\zeta_1(k)]_{k=k^*} = \frac{1}{2}\frac{d}{dk}\left[\frac{r}{1 + ky^*} - 2mx^* - d - \frac{acy^*}{(a + x^*)^2} + r_1 - \frac{2fy^*}{b + x^*}\right]_{k=k^*}$$
$$= -\frac{ry^*}{2(1 + k^*y^*)^2} \neq 0.$$

Hence, completes the proof. □

6.2. For fractional order system

6.2.1. Hopf-bifurcation analysis

In fractional order system we have examined the conditions of Hopf-bifurcation analytically for the occurrence of the same. In reality, if oscillation occurs periodically and the density of both the species prey and predator dies out or vanishes or begin to fluctuate, then Hopf-bifurcation may occur. The system (2.9) shows Hopf-bifurcation close to the interior steady state E_s^*. The given system goes to Hopf-bifurcation w.r.t. the parameters k (fear factor) and α (fractional order). We have defined the fractional order system as:

$$ {}_{t_0}^{C}D_t^{\alpha} x(t) = \mathbb{A}\left(\tau, x(t)\right), \quad \text{where} \quad x \in R^2 \quad \text{and} \quad 0 < \alpha < 1. \tag{6.1} $$

Let the system undergoes to Hopf-bifurcation near the co-existence point E_s^* w.r.t. the parameter τ at $\tau = \tau^*$ if

(i) the variational matrix at the co-existence point E_s^* of (6.1) has a pair of imaginary conjugate eigenvalues $\lambda_{1,2} = h_j \pm iw_j$ reduces to purely imaginary at $\tau = \tau^*$,

(ii) $\mho_{1,2}(\alpha, \tau^*) = 0$ and

(iii) $\dfrac{\partial \mho_{1,2}}{\partial \tau}|_{\tau=\tau^*} \neq 0$,

where $\mho_i(\alpha, \tau) = \dfrac{\alpha\pi}{2} - \min_{i=1,2} |\arg(\lambda_i(\tau))|$. From previous portion, it has been investigated that α of FOD shows a vital role and it is controlled the stability of the dynamics of this model. Then, the model system (6.1) may undergoes Hopf-bifurcation w.r.t. the model parameter α which has been presented as bellow:

(i) at the co-existence point E_s^*, a pair of imaginary conjugate eigenvalues corresponding the variational matrix of (6.1) are $\lambda_{1,2} = \alpha_j \pm iw_j$ become to purely complex number at $\alpha = \alpha^*$,

(ii) $\Psi_{1,2}(\alpha^*) = 0$ and

(iii) $\dfrac{\partial \Psi_{1,2}}{\partial \tau}|_{\alpha=\alpha^*} \neq 0$,

where $\Psi_i(\alpha) = \dfrac{\alpha\pi}{2} - \min_{i=1,2} |\arg(\lambda_i(\alpha))|$. In the following theorem, we define the restriction of Hopf-bifurcation of the above said model (2.9).

Theorem 6.3. *Around the co-existence point $E_{s^*}(x^*, y^*)$ the model system* (2.9) *undergoes Hopf-bifurcation at $\alpha = \alpha^* = \tan^{-1}\left(\dfrac{e_{15}}{e_{13}}\right)$, where $4e_{14} > e_{13}^2, e_{13} \neq 0$.*

Proof. Now, from (5.4) we get

$$ \lambda_{1,2} = \gamma_1 \pm \gamma_2, \gamma_1 = \frac{e_{13}}{2} > 0 \ \ \& \ \ \gamma_2 = \frac{e_{15}}{2}. $$

$$ \Psi_{1,2}(\alpha) = \frac{\alpha\pi}{2} - \min_{i=1,2} |\arg(\lambda_i)|, $$

$$ \Psi_{1,2}(\alpha^*) = \frac{\alpha^*\pi}{2} - \tan^{-1}\left(\frac{\gamma_2}{\gamma_1}\right) = \tan^{-1}\left(\frac{\gamma_2}{\gamma_1}\right) - \tan^{-1}\left(\frac{\gamma_2}{\gamma_1}\right) = 0. $$

Hence, we have

$$\left.\frac{\partial \Psi_{1,2}}{\partial \alpha}\right|_{\alpha=\alpha^*} = \frac{\pi}{2} \neq 0.$$

So, every conditions of Hopf-bifurcation are satisfied. Here, the system undergoes to Hopf-bifurcation w.r.t. the parameters k and α. Analytically, it is not possible to find out the critical values of another parameters such as fear level (k) and (f). Numerically, we have observed that some important crucial parameters of this model plays a innovative role where the system (2.9) undergoes to Hopf-bifurcation and trans-critical bifurcation. □

7. Numerical simulations and discussions

In this section, we will validate our analytical findings numerically. In this regard, MATLAB, Mathematica and Matcont are the key software used for this purpose. To know the system dynamics, we will use the set of parameter values as reported in Table 2 throughout this article. Taking this set of parameter values, we have formu-

Table 2. Parameter set

Parameters	Values	Sources
r	0.3	Assumed
k	0.1	Assumed
m	0.01	Assumed
c	0.1	Assumed
r_1	0.05	Assumed
a	1	Assumed
d_1	0.01	Assumed
f	0.04	Assumed
b	1	Assumed

lated all the fixed points as trivial equilibrium point $E_0(0,0)$, prey free equilibrium point $E_1(0,1.25)$, predator free equilibrium point $E_2(29,0)$ and the co-existence equilibrium point $E^*(4.40447, 6.75559)$. Now, it is necessary to check the stability of our proposed system around these fixed points. For this sake, we have computed all eigenvalues of the Community matrix corresponding to the fixed points to determine the stability scenario near each of these equilibrium points. The nature of each equilibrium point is described in Table 3 as follows:

Table 3. Nature of each equilibrium point

Equilibrium point	Eigenvalues	Nature
$E_0(0,0)$	$\lambda_1 = 0.05, \lambda_2 = 0.29$	unstable
$E_1(0,1.25)$	$\lambda_1 = -0.29, \lambda_2 = 0.05$	unstable
$E_2(29,0)$	$\lambda_1 = -0.05, \lambda_2 = 0.131667$	unstable
$E^*(4.40447, 6.75559)$	$\lambda_{1,2} = 0.00390866 \pm 0.0467694i$	unstable

Note: If there are more than one picture in any figure, then we will call the 1st picture in 1st row 1st column as **Fig.a**, 2nd picture in 1st row 2nd column as **Fig.b**,

3rd picture in 2nd row 1st column as **Fig.c**, 4th picture in 2nd row 2nd column as **Fig.d**. This process will be continued for all figures.

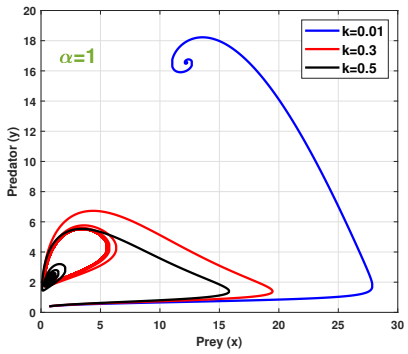

Figure 1. Presentation of different dynamical behaviour of the model system for $\alpha = 1$ by considering different value of fear level k. The system dynamics exhibits stable scenario for $k = 0.01$ which has been plotted by blue lines; for $k = 0.3$ it shows unstable scenario through periodic oscillation (see red curve) while for $k = 0.5$ it illustrates stable scenario by washing out the periodic oscillations.

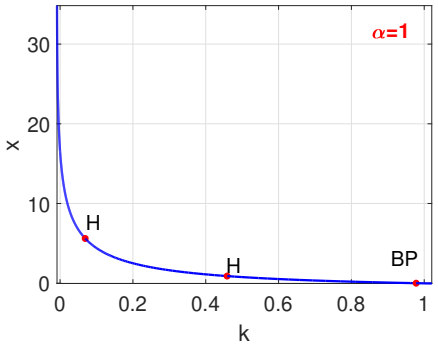

Figure 2. Occurrence of multiple Hopf-bifurcation w.r.t fear level k in $[0, 1]$ for $\alpha = 1$. The first Hopf point occurs for $k = k^* = 0.069$ while the second Hopf point occurs for $k = k^* = 0.458709$.

Now, we will investigate the dynamical behaviour of our proposed system with respect to some crucial parameters one by one. In this context, first we will vary the level of fear. For $k = 0.01$, the system shows stable scenario around the interior point $E^*(12.24, 16.55)$ as the eigenvalues of the Jacobian matrix at this point are $\lambda_{1,2} = -0.0284204 \pm 0.0728853i$ and the corresponding phase portrait is shown in Fig.1 by blue line; for $k = 0.3$ the system shows unstable scenario (see Fig.1 red curve) around the interior point $E^*(1.62321, 3.27902)$ as the eigenvalues of the Jacobian matrix at this point are $\lambda_{1,2} = 0.005558 \pm 0.0279414i$; interestingly for further increase of fear level, i.e., for $k = 0.5$ the system shows stable scenario (see Fig.1 black curve) near $E^*(0.764902, 2.20613)$ as the eigenvalues are $\lambda_{1,2} = -0.00173738 \pm 0.0194793i$. However, it is observed that at low level of fear the system shows stable scenario, for moderate value of fear the system shows unstable scenario by producing limit cycle oscillation and for high level of fear the system shows stable scenario by removing the limit cycle oscillation. Therefore, our proposed system undergoes two Hopf-bifurcations as shown in Fig.2. The bifurcation diagrams are shown in

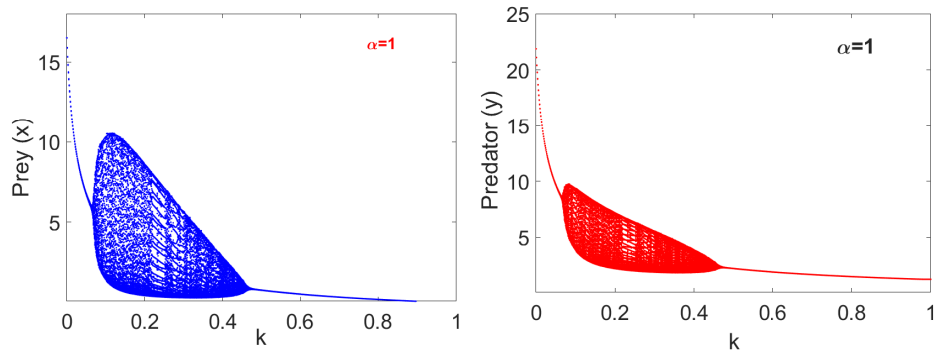

Figure 3. Plot of bifurcation diagram w.r.t k in $[0, 1]$ for $\alpha = 1$. The model system shows stable scenario for $k < k^* = 0.069$, but for $k \in [0.069,\ 0.458]$ it shows oscillatory scenario. Interestingly for further increase in fear level k the system becomes stable.

Fig.3 which clarifies that the system remains stable until it crosses the threshold parametric limit $k = k^* = 0.069$ and after crossing this threshold parametric limit it enters into an unstable zone and it becomes stable again when it crosses the threshold parametric limit $k = k^* = 0.458709$. For further increase of fear level the system remains stable but the prey population goes to extinction (see Fig.3a). In addition, we have computed the 1st Lyapunov coefficient (l_1) to determine the direction and stability of Hopf-bifurcation. It is observed that at $k = k^* = 0.069$ the 1st Lyapunov coefficient (l_1) is -0.0004008163 which indicates that the bifurcation is super-critical and the bifurcating periodic solution is stable as negativity of 1st Lyapunov coefficient (l_1) implies the occurrence of super-critical Hopf-bifurcation along with orbitally stable bifurcating limit cycle and the period of the bifurcating limit cycle increases with the increase of fear level k as shown in Fig.4. Now, at the second Hopf point $k = 0.458709$ the 1st Lyapunov coefficient (l_1) is -0.005273313 which consequently indicates the occurrence of super-critical Hopf-bifurcation with stable bifurcating limit cycle and the period increases with the increase of fear level up to the threshold value $k = k^* = 0.458709$ (see Fig.4). Moreover, at this Hopf point the limit cycle bifurcates and a limit point cycle (LPC) occurs. To confirm

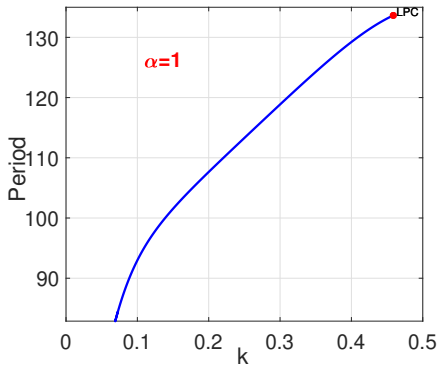

Figure 4. Relation between period of the bifurcating limit cycle with fear level k for $\alpha = 1$. It is noticed that period of the bifurcating limit cycle increases with the increase of fear level.

the stability of bifurcating limit cycle we have drawn the modulus of all Floquet

multipliers with fear parameter k and it is observed that modulus of one Floquet multiplier is always one (due to rotation) and other one is less the 1, as shown in Fig.5(a) (for first Hopf point) and Fig.5(b) (for second Hopf point) which reveals that the bifurcating limit cycles are stable.

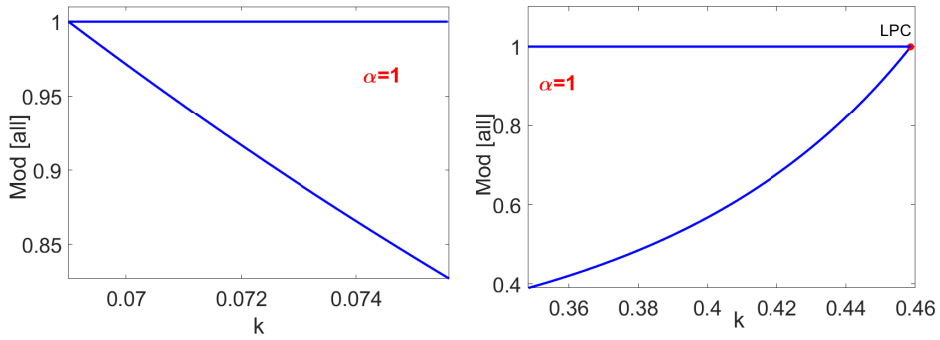

Figure 5. Exhibits stability of limit cycle oscillation for different values of k based on the properties of Floquet multipliers for $\alpha = 1$. Here, modulus of one Floquet multiplier is one and other one is less than one and hence the limit cycle oscillation is stable.

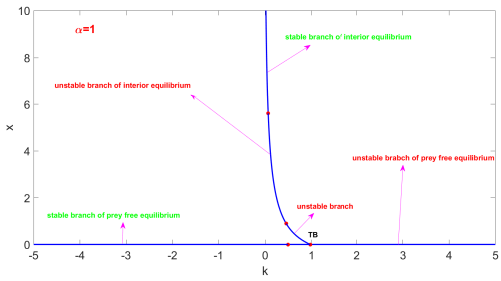

Figure 6. Transcritical bifurcation diagram w.r.t k for the integer order model system.

Moreover, it is illustrated that a Transcritical bifurcation occurs around the prey free equilibrium point $E_1(0, 1.25)$ for $k = k^* = 0.977778$ as shown in Fig.6. Now, we have considered the oscillatory phenomenon of the model system by choosing $k = 0.3$ to observe the influence of fractional order α in the system dynamics keeping other parameters fixed as of (2). Here, we have investigated that the proposed system demonstrates unstable scenario by producing limit cycle oscillation for $\alpha = 0.99, \alpha = 0.96, \alpha = 0.94$ as shown in Fig. 7(a), (b), (c) respectively. Interestingly, for further decrease in the value of $\alpha = 0.92$ we have noticed that the system dynamics becomes stable by removing the periodic oscillation. So, we can conclude that fractional order α has stabilizing effect in the system dynamics irrespective of the value of fear parameter k and the model system experiences Hopf bifurcation w.r.t. this fractional order α. To visualize the role of α we have plotted Hopf-bifurcation diagram w.r.t. α in the range $\alpha \in [0.8, 1]$. Fig.8(a) reveals the fact that there is a enough difference between max (prey population density) and min (prey population density) which consequently creates the unstable situation for prey species in the range $\alpha \in [0.8, 1]$ and the same is true for predator species also. Interestingly, a slight decrements in α, i.e., for $\alpha \in (0, 0.8)$ it is observed that both the population

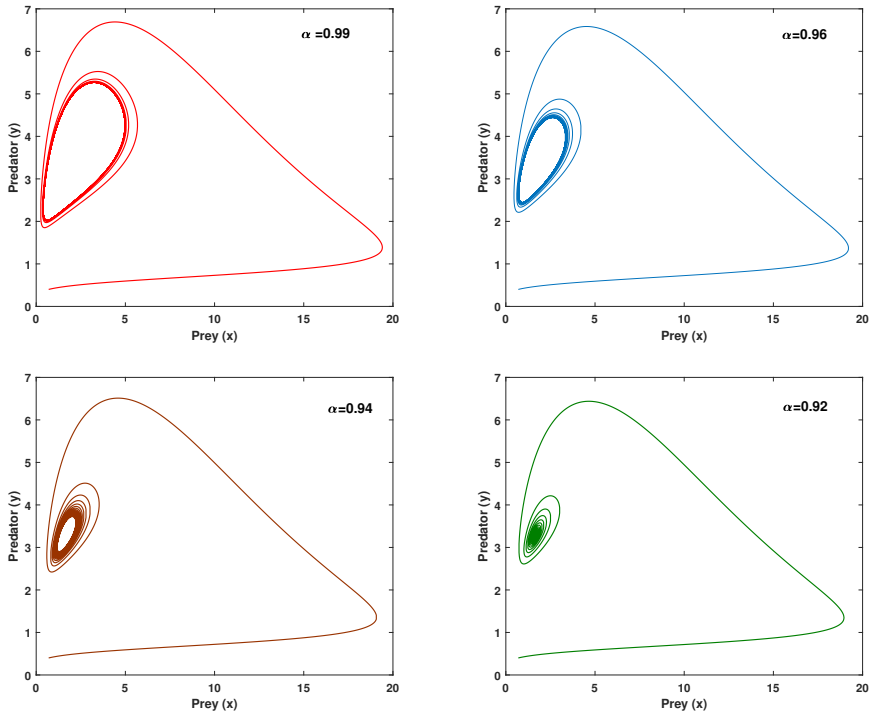

Figure 7. Phase portrait diagram under different values of α for predator induced fear $k = 0.3$. It is examined that reduction in α makes the model system stable.

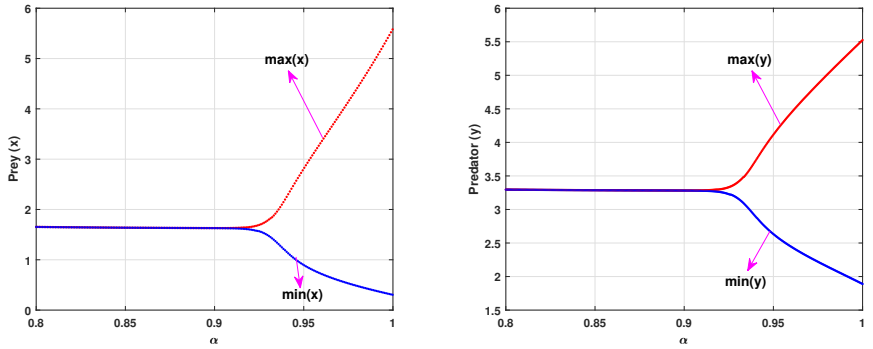

Figure 8. Bifurcation diagram w.r.t α by taking $k = 0.3$ and remaining other parameters same as above. It is examined that for the threshold value of fractional order $\alpha > \alpha^* = 0.945$ the model system exhibits unstable scenario by making sufficiently large difference between maximum and minimum of both the population density while slight decrements in α makes the system dynamics stable by making maximum and minimum of both the population density same.

density do not fluctuate, i.e., maximum of population density and minimum of population density coincides with each other and produces a stable scenario for the model system. Here, it may be concluded that reduction in α makes the system stable and the reason may be interpreted as follows:

Since fractional order differential equation catches all the past performance of

species and hence prey species may adapt different defensive strategy in response to predator attack which consequently increases their population density. Again, we have plotted mean density of both the population under the variation of α by fixing $k = 0.3$. It is examined that the density of prey and predator population increases in the range $0 < \alpha \leq 0.4$ and $0 < \alpha \leq 0.55$. But, surprisingly, when α crosses 0.4 (for prey) and 0.55 (for predator) then both the population mean density begins to decrease and eventually fluctuates when α just crosses the threshold parametric limit $\alpha = \alpha^* = 0.945$. Now, we will focus on f to know the role of the

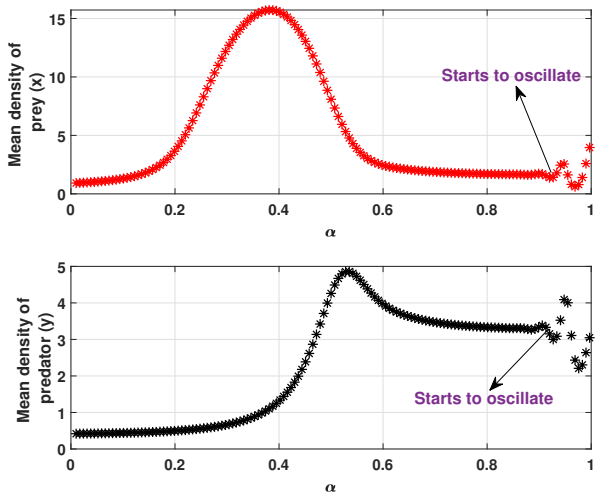

Figure 9. Plot of change in mean population biomass of both the species under the variation of model parameter α considering $k = 0.3$. It is observed that both prey and predator population start to oscillate when α just crosses the threshold parametric limit $\alpha = \alpha^* = 0.945$. For $0 < \alpha \leq 0.4$ mean density of prey species persistently increases and then in the range $0.4 < \alpha \leq 0.65$ it decreases while predator population biomass continuously increases in the range $0 < \alpha \leq 0.55$.

parameter f in the system dynamics. For this, first we have taken $f = 0.04$ and investigated that around the interior co-existence steady state $E^*(4.40447, 6.75559)$ the system exhibits unstable scenario by producing limit cycle as shown in Fig.10 since the eigenvalues at this points are $\lambda_{1,2} = 0.00390866 \pm 0.0467694i$. Interestingly, when we increase the value of f, i.e., for $f = 0.07$ the limit cycle not appears and the model system displays stable scenario near the co-existence point $E^*(9.20729, 7.29092)$ (see Fig.10B) as the eigenvalues obtained at this point are $\lambda_{1,2} = -0.0388211 \pm 0.0556468i$. Moreover, for lower value of the system shows stable scenario and the system undergoes multiple Hopf-bifurcations as shown in Fig. 11. The bifurcation diagram w.r.t f are displayed in Fig.12. It clarifies that the proposed model exhibits stable scenario in the interval $f \in [0, 0.022787)$ and becomes unstable by occurring a Hopf bifurcation at $f = f^* = 0.022787$ and remains unstable in the interval $f \in [0.022787, 0.04211]$. For, $f > 0.04211$ the system shows stable scenario. Moreover, we have calculated 1st Lyapunov coefficient (l_1) at both the Hopf points. At $f = f^* = 0.022787$, the 1st Lyapunov coefficient becomes $l_1 = -0.009616536$ which specify the occurrence of super-critical Hopf-bifurcation with stable bifurcating limit cycle. At the second Hopf point which occurs at $f = f^* = 0.04211$ the 1st lyapunov coefficient l_1 becomes -0.000521551

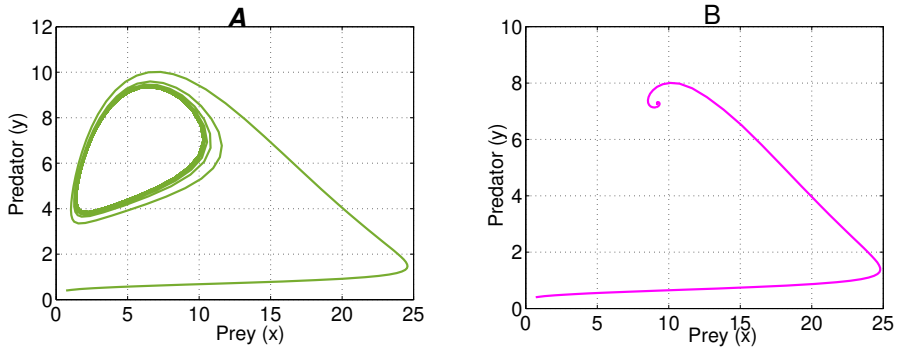

Figure 10. Phase portraits plot of the system for $\alpha = 1$. Fig.A exhibits the limit cycle oscillation for $f = 0.04$; Fig.B displays the disappearance of limit cycle oscillation for $f = 0.07$

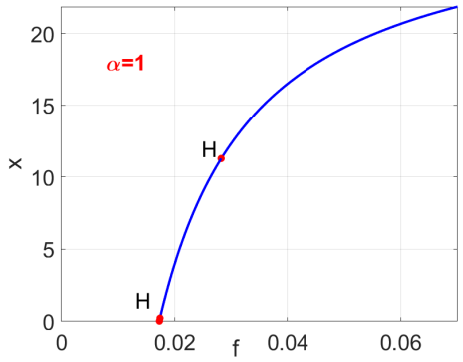

Figure 11. Occurrence of multiple Hopf-bifurcation w.r.t f for the integer order model system.

which implies that a super-critical Hopf bifurcation occurs with orbitally stable limit cycle. In addition, to confirm the stability of produced limit cycles we have plotted diagrams of Floquet multipliers vs f (see Fig.13) at those hopf points and observed that modulus of one multiplier is always one (due to rotation) and the value of the other modulus lies below the quantity 1 which consequently guarantee's the stability of limit cycle.

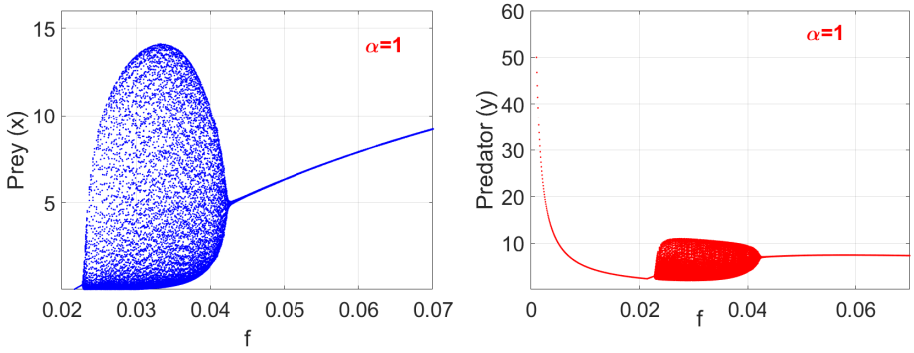

Figure 12. Bifurcation diagram w.r.t f for the integer order model system.

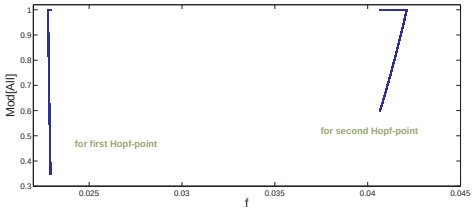

Figure 13. Stability of limit cycle oscillation w.r.t f for the integer order model system.

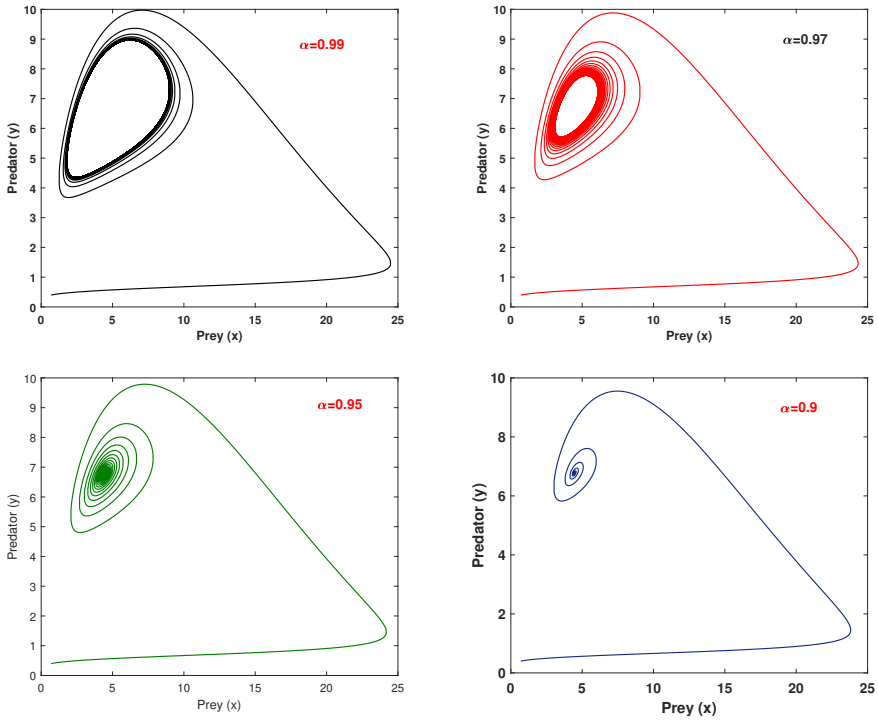

Figure 14. Phase portrait diagram under different values of α for $f = 0.04$ keeping other parameter same as above. We have examined that reduction in α makes the model system stable.

Now, to check the impact of the system dynamics under the variation of fractional order α we have considered the unstable scenario by choosing $f = 0.04$ and observed different dynamical nature for different values of α. For $\alpha = 0.99$ and $\alpha = 0.97$ the model system exhibits limit cycle oscillation (see Fig.14(a)and (b)). But, slight reduction in α, i.e., for $\alpha = 0.95$ it displays stable behavior (see 14(c)) by eliminating periodic oscillation and this phenomena continues for further reduction in α (see Fig.14(d)). So, we can conclude that the model system undergoes a Hopf-bifurcation w.r.t. this fractional order α and this scenario has been portrayed in Fig.15. From Fig.15, it is noticed that the system remains stable for $\alpha < \alpha^* \leq 0.95$ and becomes unstable behavior by producing periodic oscillation whenever α just crosses the threshold parametric limit $\alpha = \alpha^* = 0.95$. Again, we have checked the amount of mean density under the variation of α in $\alpha \in (0, 1]$ which has been portrayed in Fig.16. From Fig.16, it is clear that, for $0 < \alpha \leq 0.4$ prey population

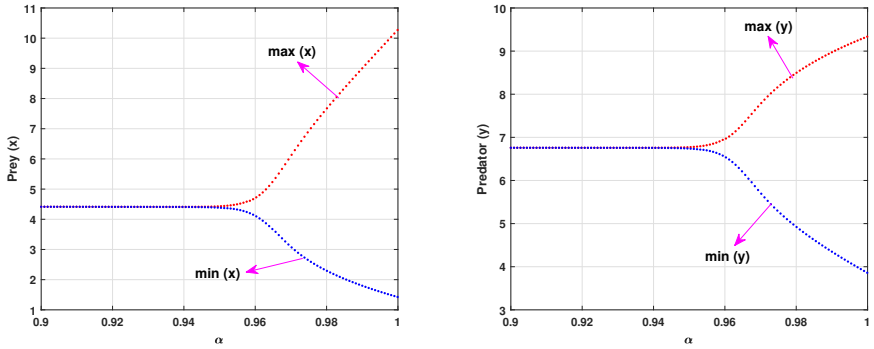

Figure 15. Bifurcation diagram w.r.t α for $f = 0.04$ in $\alpha \in [0, 1]$. It reveals the fact that for $\alpha \in [0.95, 1]$ the model system exhibits unstable scenario by producing periodic oscillation of both the population density (existence of maximum and minimum population density), however, slight reduction in α makes the system free from periodic oscillation and hence displays stable scenario.

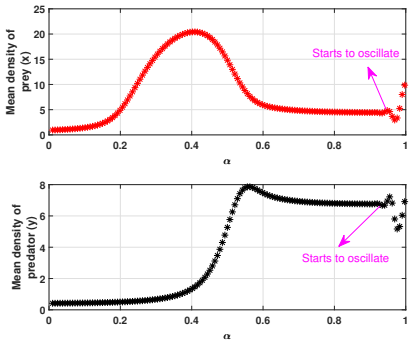

Figure 16. Plot of change in mean population biomass of both the species under the variation of model parameter α for $f = 0.04$. It is observed that both prey and predator population start to oscillate when α just crosses the threshold parametric value $\alpha = \alpha^* = 0.95$. For $0 < \alpha \leq 0.4$ mean density of prey species persistently increases and then in the range $0.4 < \alpha \leq 0.65$ it decreases while predator population biomass continuously increases in the range $0 < \alpha \leq 0.55$.

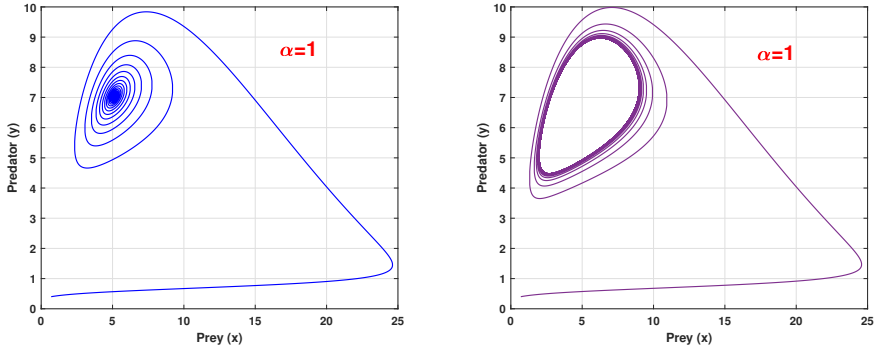

Figure 17. Phase portraits plot of the system for $\alpha = 1$. The system dynamics exhibits stable scenario for $b = 0.5$ as shown in Fig.a; but for $b = 0.9$ it shows unstable scenario by producing periodic oscillation as displayed in Fig.b.

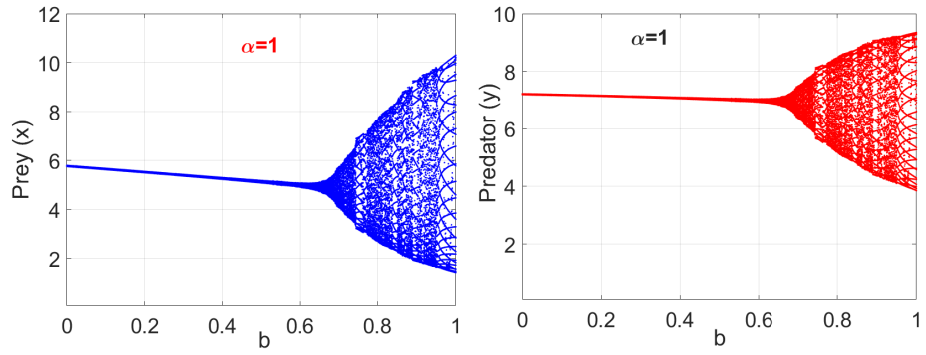

Figure 18. Bifurcation diagram w.r.t b in $[0, 1]$ for the integer order model system. It is examined that the model system shows locally asymptotically stable scenario until b exceeds the threshold value $b = b^* = 0.707356$; whenever b just crosses this threshold parametric limit $b = b^* = 0.707356$ then the system dynamics changes its qualitative scenario from stable to unstable and it continues for further increase in b.

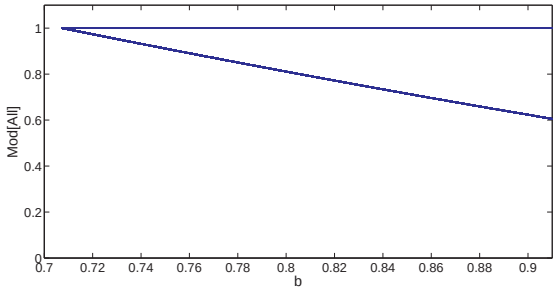

Figure 19. Stability of limit cycle oscillation through the plot of Floquet multipliers for the integer order counterpart system. Here, it is observed that out of two Floquet multipliers one is always 1 and the other one is less than 1 which consequently reveals that the limit cycle oscillations are stable.

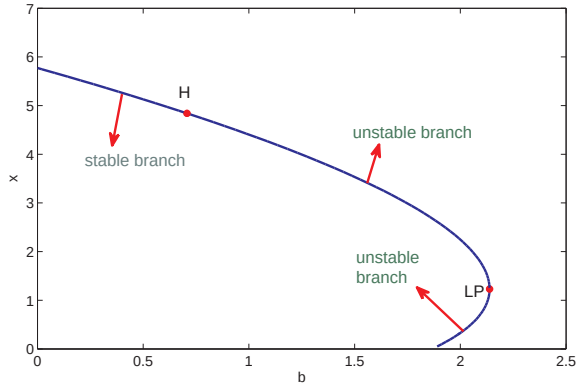

Figure 20. Saddle-node bifurcation for $b = 2.13$ for the integer order counterpart system.

mean biomass increase ; for $0.4 < \alpha \leq 0.65$ it decreases and at last for $\alpha > 0.95$ it begins to oscillate. However, predator population mean biomass continuously increases in the range $\alpha \in (0, 0.55]$ and decreases slightly until α just crosses the

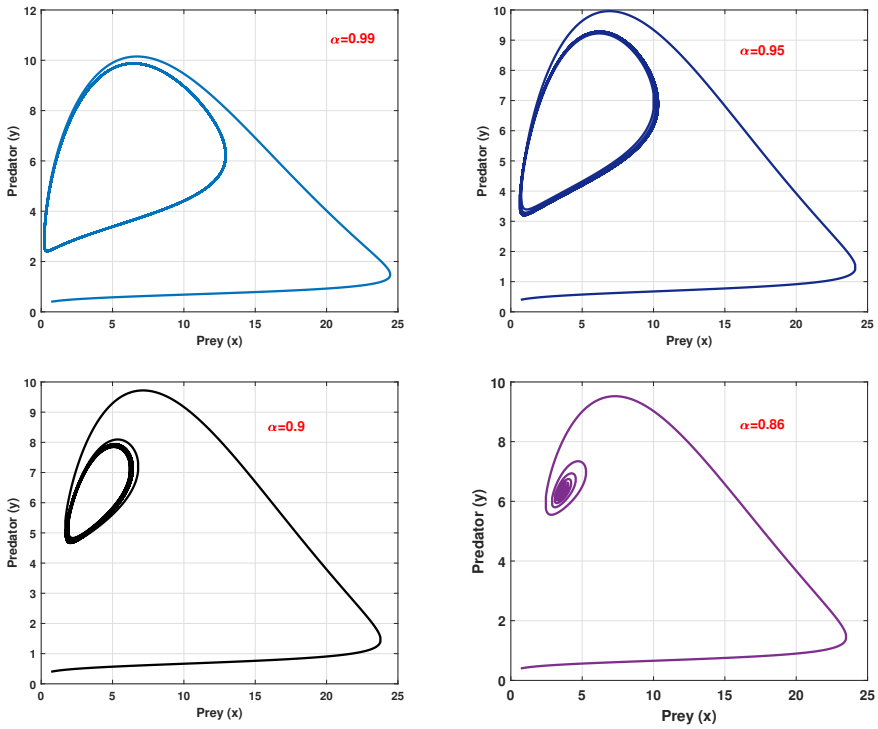

Figure 21. Phase portrait diagram under different values of α for $b = 1.5$ keeping other parameters same as above. It is examined that reduction in α makes the model system stable for $b = 1.5$.

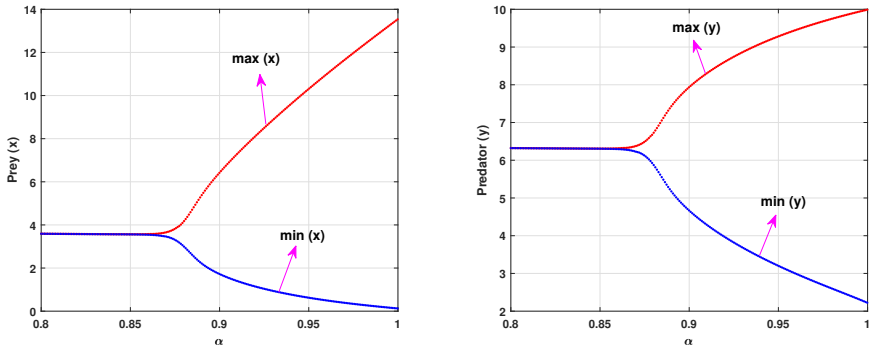

Figure 22. Bifurcation diagram w.r.t α for $b = 1.5$ in $\alpha \in [0, 1]$. It reveals the fact that for $\alpha \in [0.86, 1]$ the model system exhibits unstable scenario by producing periodic oscillation of both the population density (existence of maximum and minimum population density), however, slight reduction in α makes the system free from periodic oscillation and hence displays stable scenario.

threshold parametric limit $\alpha = \alpha^* = 0.95$. So, it can be easily concluded that fractional order α has a deep impact not only on the stability of the system dynamics but also on mean population biomass. Now, we are interested to know the system dynamics with the variation of the parameter b. For $b = 0.5$ the system becomes stable and the corresponding phase portrait is given in Fig.17a and for $b = 0.9$ the model system demonstrates unstable scenario near the interior coexistence steady

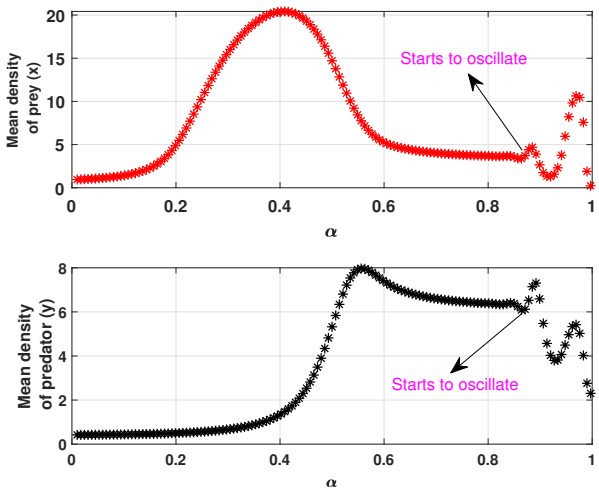

Figure 23. Plot of change in mean population biomass of both the species under the variation of model parameter α considering $b = 1.5$. It is observed that both prey and predator population start to oscillate when α just crosses the threshold parametric limit $\alpha = \alpha^* = 0.86$. For $0 < \alpha \leq 0.4$ mean density of prey species persistently increases and then in the range $0.4 < \alpha \leq 0.6$ it decreases while predator population biomass continuously increases in the range $0 < \alpha \leq 0.55$.

state $E_1^*(6.82258, 4.55807)$ by producing limit cycle as shown in Fig.17b since the eigenvalues at this point are obtained as $\lambda_{1,2} = 0.0274764 \pm 0.0246072i$. The bifurcation diagrams are displayed in Fig.18 which tells that the system becomes unstable from its locally asymptotically stable situation when it just crosses the threshold parametric limit $b = b^* = 0.707356$. Further, we have formulated the 1st Lyapunov coefficient as $l_1 = -0.0006112797$ which indicates that the Hopf-bifurcation is super-critical with orbitally stable limit cycle. Moreover, the stability of limit cycle is confirmed from Fig.19 as the modulus of Floquet multipliers becomes ≤ 1. In addition, a limit point (LP) bifurcation is detected by MATCONT at $b = 2.138399$ with nonzero normal form coefficient -0.01026175 which indicates that a orbitally stable limit cycle may bifurcate around the point $E^*(1.232014, 4.213015)$. The bifurcation diagram is shown in Fig.20 and a neutral saddle point $(0.320041, 2.896456)$ occurs for $b = 1.997124$. Again, to check the impact of the fractional order α we have considered the periodic oscillation situation of the model system by taking $b = 1.9$. We have observed that continuous reduction in α forces the system to exhibit stable behavior. The system shows unstable behavior for $\alpha = 0.99,\ 0.95,\ 0.9$ as shown in Fig.21(a),(b),(c) respectively. But, for $\alpha = 0.86$ the system exhibits stable behavior by washing out the periodic oscillation as displayed in Fig.21(d). So, it is obvious that the model system undergoes Hopf-bifurcation w.r.t. α which has been reflected in Fig.22. From Fig.22, it is noticed that the system remains stable for $\alpha < \alpha^* \leq 0.86$ and becomes unstable behavior by producing periodic oscillation whenever α just crosses the threshold parametric limit $\alpha = \alpha^* = 0.86$. At last, we have plotted the mean density diagram to predict the role of α in population density as displayed in Fig.23. It is examined that both prey and predator population start to oscillate when α just crosses the threshold parametric limit $\alpha = \alpha^* = 0.86$. For $0 < \alpha \leq 0.4$ mean density of prey species persistently increases and then in the

range $0.4 < \alpha \leq 0.6$ it decreases while predator population biomass continuously increases in the range $0 < \alpha \leq 0.55$.

8. Conclusion

In this article, a modified Leslie-Gower predator-prey scheme with predator induced fear in fractional sense has been proposed. The well-posedness of the proposed system has been studied rigorously. It is observed when the system reaches to both predator and prey free equilibrium steady state then it always displays unstable scenario near the fixed point. Biologically, the system can never be stable at the zero equilibrium state. The system possesses one predator free equilibrium state and under the feasibility condition of existence of the equilibrium state it always exhibits unstable scenario. For the logistic type growth term of the predator species, the system may reach to one prey free equilibrium state. Depending upon the parametric constraints it may either exhibits stable scenario or unstable scenario. It is investigated that the model system experiences trans-critical bifurcation if we vary the fear parameter k as the bifurcation parameter. The system may exhibit stable co-existence or oscillatory scenario which critically depends on both fear parameter k and the memory of the individuals (α) gained from their life cycle. It is observed that when the individual has less memory, then the fear level (k) stabilizes the predator-prey system via two consecutive Hopf-bifurcation. It has been shown numerically by calculating the 1st Lyapunov coefficient at the bifurcation points that the first occurrence of Hopf-bifurcation is super critical and the produced limit cycle shows stable scenario and for enhancement in the fear level the period of the limit cycle increases; the second Hopf-bifurcation occurs for further development of fear level and this time through saddle-node bifurcation of limit cycle (LPC occurs at the second Hopf point) a stable steady state occurs. Memory of species may play vital role in states of stability of the regarding system. It is observed, that the order α (measures memory of the species) of the fractional order system is inversely proportional in case of stabilizing the system. That is, decreasing value of α stabilizes the system whether incremental α fosters destabilization of the system. As the lower value of α refers to strong memory of the interacting species; then it may be concluded that when the intervening species of our model system are able to memorize the past then it leads to stable co-existence of the species. On the other hand, fading memory may be a possible reason for periodic co-existence of the species (all the facts have been numerically checked). This study uncovers some useful results on impact of forgetting process of interacting species when a particular species is driven by indirect effect. It is to be noted that, we consider homogeneous distribution of species; in case of in homogeneity in spatial distribution, the process of memorizing the previous facts may have different outcomes on the evolution of the species. This gap may be covered in future studies.

Acknowledgements. The researchers would like to thank the Deanship of Scientific Research, Qassim University for funding the publication of this project.

References

[1] S. Alam, *Risk of disease-selective predation in an infected prey-predator system*, Journal of Biological Systems, 2009, 17(1), 111–124.

[2] M. A. Aziz-Alaoui and M. Daher Okiye, *Boundedness and global stability for a predator–prey model with modified Leslie–Gower and Holling-type II schemes*, Appl. Math. Lett., 2003, 16, 1069–1075.

[3] A. Altan and R. Hacıoglu˘, *Model predictive control of three-axis gimbal system mounted on uav for real-time target tracking under external disturbances*, Mech. Syst. Signal Process, 2020, 138. DOI: 10.1016/j.ymssp.2019.106548.

[4] A. Altan, S. Karasu and S. Bekiros , *Digital currency forecasting with chaotic meta-heuristic bio-inspired signal processing techniques*, Chaos, Solitons & Fractals, 2019, 126, 325–336.

[5] E. Ahmed, A. El-Sayed and H. A. El-Saka, *Equilibrium points, stability and numerical solutions of fractional-order predator–prey and rabies models*, J. Math. Anal. Appl., 2007, 325(1), 542–553.

[6] A. Atangana and A. Secer, *A note on fractional order derivatives and table of fractional derivatives of some special functions*, Abstract and applied analysis, Hindawi. Doi:101155/2013/279681 (2013).

[7] J. Alidousti and E. Ghafari, *Dynamic behavior of a fractional order prey-predator model with group defense*, Chaos, Solitons & Fractals, 2020, 134, 109688. Doi:10.1016/j.chaos.2020.109688.

[8] M. M. Amirian, I. Towers, Z. Jovanoski and A. J. Irwin, *Memory and mutualism in species sustainability: A time-fractional Lotka-Volterra model with harvesting*, Heliyon, 2020, 6(9). Doi:10.1016/j.heliyon.2020.e04816.

[9] D. Baleanu, A. Jajarmi, S. S. Sajjadi and J. H. Asad, *The fractional features of a harmonic oscillator with position-dependent mass*, Commun. Th. Phys., 2020, 72(5), 055002. Doi:10.1088/1572-9494/ab7700.

[10] D. Barman, J. Roy, H. Alrabaiah, P. Panja, S. P. Mondal and S. Alam, *Impact of predator incited fear and prey refuge in a fractional order prey predator model*, Chaos, Solitons and Fractals, 2020, 142(1). DOI:10.1016/j.chaos.2020.110420.

[11] D. Barman, J. Roy and S. Alam, *Dynamical scenario of an Infected Predator-Prey Model with Fear Effect*, Iranian Journal of Science and Technology, Transactions A: Science, 2020, 45(5721). DOI:10.1007/s40995-020-01014-y.

[12] D. Barman, J. Roy and S. Alam, *Trade-off between fear level induced by predator and infection rate among prey species*, Journal of Applied Mathematics and Computing, 2020, 1–29. Doi:org/10.1007/s12190-020-01372-1.

[13] A. A. Berryman, *The origins and evolution of predator-prey theory*, Ecology, 1992, 75, 1530–1535.

[14] F. Chen, L. Chen and X. Xie, *On a Leslie–Gower predator–prey model incorporating a prey refuge*, Nonlinear Anal Real World Appl, 2009, 10(5), 2905–2908. DOI:10.1016/j.nonrwa.2008.09.009.

[15] C. W. Clark, *Mathematical models in the economics of renewable resources*, SIAM Rev., 1979, 21, 81–99.

[16] W. Cresswell, *Predation in bird populations*, J. Ornithol, 2011, 152, 251–263.

[17] S. Creel and D. Christianson, *Relationships between direct predation and risk effects*, Trends Ecol. Evolut., 2008, 23, 194–201.

[18] S. Creel, D. Christianson, S. Liley and J. A. Winnie, *Predation risk affects reproductive physiology and demography of elk*, Science, 2007, 315(5814), 960. DOI:10.1126/science.1135918 (2007).

[19] T. Das, R. N. Mukherjee and K. S. Chaudhari, *Bioeconomic harvesting of a prey–predator fishery*, J. Biol. Dyn., 2009, 3, 447–462.

[20] Y. Du, R. Peng and M. Wang, *Effect of a protection zone in the diffusive Leslie predator–prey model*, J. Differ. Equ., 2009, 246, 3932–3956.

[21] V. D. Djordjevic´, J. Jaric´, B. Fabry, J. J. Fredberg and D. Stamenovic´, *Fractional derivatives embody essential features of cell rheological behavior*, Ann. Biomed Eng., 2003, 31(6), 692–699.

[22] A. Dokoumetzidis, R. Magin and P. Macheras, *A commentary on fractionalization of multi-compartmental models*, Journal of pharmacokinetics and pharmacodynamics, 2010, 37(2), 203–207.

[23] H. I. Freedman, *Deterministic Mathematical Models in Population Ecology*, Marcel Dekker, New York, 1980.

[24] R. P. Gupta and P. Chandra, *Bifurcation analysis of modified Leslie–Gower predator–prey model with Michaelis–Menten type prey harvesting*, J. Math. Anal. Appl.,2013, 398, 278–295.

[25] A. Jajarmi and D. Baleanu, *A new iterative method for the numerical solution of high-order non-linear fractional boundary value problems*, Front. Phys., 2020, 8, 220. Doi:10.3389/fphy.2020.00220.

[26] Q. Khan, E. Balakrishnan and G. Wake, *Analysis of a predator-prey system with predator switching*, Bull. Math. Biol., 2004, 66(1), 109–23.

[27] S. Khajanchi, *Modeling the dynamics of stage-structure predator-prey system with Monod–Haldane type response function*, Applied Mathematics and Computation, 2017, 302(1),122–143. https://doi.org/10.1016/j.amc.2017.01.019.

[28] S. Khajanchi and S. Banerjee, *Role of constant prey refuge on stage structure predator–prey model with ratio dependent functional response*, Applied Mathematics and Computation, 2017, 314, 193–198. Doi.org/10.1016/j.amc.2017.07.017.

[29] S. Khajanchi, *Dynamic behavior of a Beddington–DeAngelis type stage structured predator–prey model*, Applied Mathematics and Computation, 2014, 244, 344–360. Doi:org/10.1016/j.amc.2014.06.109.

[30] L. Kexue and P. Jigen, *Laplace transform and fractional differential equations*, Applied Mathematics Letters, 2011, 24(12), 2019–2023.

[31] S. Liang, R. Wu and L. Chen, *Laplace transform of fractional order differential equations*, Electron. J. Differ. Equ., 2015, 139, 1–15.

[32] Y. Li, Y. Chen and I. Podlubny, *Mittag–leffer stability of fractional order nonlinear dynamic systems*, Automatica, 2009, 45(8), 1965–1969.

[33] S. Liu and E. Beretta, *A stage-structured predator-prey model of beddington-deangelis type*, SIAM J. Appl. Math., 2006, 66(4), 1101–1129.

[34] P. H. Leslie, *A stochastic model for studying the properties of certain biological systems by numerical methods*, Biometrika, 1958, 45, 16–31.

[35] P. H. Leslie and J. C. Gower, *The properties of a stochastic model for the predator–prey type of interaction between two species*, BiometriKa, 1960, 47, 219–234.

[36] S. L. Lima, *Nonlethal effects in the ecology of predator-prey interactions*, Bioscience, 1998, 48, 25–34.

[37] S. L. Lima, *Predators and the breeding bird: behavioural and reproductive flexibility under the risk of predation*, Biol. Rev., 2009, 84, 485–513.

[38] X. Li and R. Wu, *Hopf bifurcation analysis of a new commensurate fractional-order hyper chaotic system*, Nonlinear Dyn., 2014, 78(1), 279–288.

[39] P. H. Leslie, *Some further notes on the use of matrices in population mathematics*, Biometrika, 1948, 35, 213–245.

[40] A. Maiti and G. P. Samanta, *Deterministic and stochastic analysis of a prey-dependent predator-prey system*, Int. J. Math. Educ. Sci. Technol., 2005, 6, 65–83.

[41] N. Mondal, D. Barman and S. Alam, *Impact of adult predator incited fear in a stage-structured prey–predator model*, Environment,Development and Sustainability, 2020, 23(6), 9280–9307. Doi.org/10.1007/s10668-020-01024-1(2020).

[42] H. Molla, S. Sarwardi and M. Sajid, *Predator-prey dynamics with Allee effect on predator species subject to intra-specific competition and nonlinear prey refuge*, Journal of Mathematics and Computer Science, 2022, 25(2), 150–165.

[43] A. K. Misra, R. K. Singh, P. K. Tiwari, S. Khajanchi and Y. Kang, *Dynamics of algae blooming: effects of budget allocation and time delay*, Nonlinear Dynamics, 2020, 100, 1779–1807.

[44] A. F. Nindjin and M. A. Aziz-Alaoui, *Persistence and global stability in a delayed Leslie-Gower type three species food chain*, J. Math. Anal. Appl., 2008, 340, 340–357.

[45] Z. M. Odibat and N. T. Shawagfeh, *Generalized taylor's formula*, Applied Mathematics and Computation, 2007, 186(1), 286–293.

[46] S. Pal, N. Pal, S. Samanta and J. Chattopadhyay, *Fear effect in prey and hunting cooperation among predators in a Leslie-Gower model*, Mathematical Biosciences and Engineering, 2019, 16, 5146–5179.

[47] I. Petra's, *Fractional-order nonlinear systems: modeling, analysis and simulation*, Springer Science and Business Media, 2011. Doi:10.1007.978-3-642-18101-6.

[48] E. Preisser, J. Orrock and O. Schmitz, *Predator hunting mode and habitat domain affect the strength of non-consumptive effects in predator–prey interactions*, Ecology, 2007, 88, 2744–2751.

[49] I. Podlubny, *Fractional differential equations of mathematics in science and engineering*. Academic Press, San Diego, Calif, USA, 1999, 198.

[50] P. Panja, *Stability and dynamics of a fractional-order three-species predator–prey model*, Theory in Biosciences, 2019, 138(2), 251–259. DOI:10.1007/s12064-019-00291-5.

[51] P. Panja, *Dynamics of a fractional order predator-prey model with intraguild predation*, Int. J. Model Simul.,2019, 39(4), 256–268.

[52] L. Perko, *Differential Equations and Dynamical Systems,* Springer Science and Business Media, 2013.

[53] J. Roy, D. Barman and S. Alam, *Role of fear in a predator-prey system with ratio-dependent functional response in deterministic and stochastic environment*, Biosystems, 2020, 197(11). DOI:10.1016/j.biosystems.2020.104176.

[54] J. Roy and S. Alam, *Study on autonomous and non-autonomous version of a food chain model with intraspecific competition in top predator*, Math. Methods Appl. Sci., 2020, 43(6), 3167–3184.

[55] J. Roy and S. Alam, *Fear factor in a prey–predator system in deterministic and stochastic environment*, Physica A: Statistical Mechanics and Its Applications, 2020, 541. Doi.org/10.1016/j.physa. 2019.123359.

[56] S. Ruan and D. Xiao, *Global analysis in a predator-prey system with non monotonic functional response*, SIAM J. Appl. Math., 2001, 61, 1445–1472.

[57] K. Sarkar and S. Khajanchi, *Impact of fear effect on the growth of prey in a predator-prey interaction model*, Ecological Complexity, 2020, 42, 100826. Doi:org/10.1016/j.ecocom.2020.100826.

[58] K. Sarkar and S. Khajanchi, *Impact of fear effect on the growth of prey in a predator-prey interaction model*, Ecological Complexity, 2020, 100826(42). Doi:org/10.1016/j.ecocom.2020.100826.

[59] K. Sarkar, S. Khajanchi, P. C. Mali and J. J. Nieto, *Rich Dynamics of a Predator-Prey System with Different Kinds of Functional Responses*, Hindawi,Complexity, 2020. https://doi.org/10.1155/2020/4285294.

[60] O. Schmitz, *Effect of predator hunting mode on grassland ecosystem function*, Science, 2008, 319, 952–954.

[61] P. K. Tiwari, R. K. Singh, S. Khajanchi, Y. Kang and A. K. Misra, *A mathematical model to restore water quality in urban lakes using Phoslock*, American Institute of Mathematical Sciences, 2021, 26(6), 3143–3175. Doi:10.3934/dcdsb.2020223.

[62] A. Wörz-Busekros, *Global stability in ecological systems with continuous time delay*, SIAM J. Appl. Math., 19788, 35(1), 123–34. Doi.org/10.1137/0135011.

[63] X. Wang, L. Zanette and X. Zou, *Modelling the fear effect in predator–prey interactions*, Journal of Mathematical Biology, 2016, 73, 1179–1204.

[64] X. Wang and X. Zou, *Modeling the Fear Effect in Predator-Prey Interactions with Adaptive Avoidance of Predators*, Bulletin of Mathematical Biology, 2017, 79, 1325–1359.

[65] J. Wang, Y. Cai, S. Fu and W. Wang, *The effect of the fear factor on the dynamics of a predator-prey model incorporating the prey refuge*, Chaos, 2019, 29, 083–109.

[66] L. Y. Zanette, A. F. White, M. C. Allen and M. Clinchy, *Perceived predation risk reduces the number of offspring songbirds produce per year*, Science, 2011, 334, 1398–1401.

[67] H. Zhang, Y. Cai, S. Fu and W. Wang, *Impact of the fear effect in a predator-prey model incorporating a prey refuge*, Applied Mathematics and Computation, 2019, 356,328–337.